

ABSTRACT

Determining the Complex Permittivity of Materials with the Waveguide-Cutoff Method

Christopher Anderson, M.S.

Randall Jean, Ph.D., P.E

A new method for the determination of complex permittivity values is explained. The Waveguide-Cutoff method consists of a rectangular chamber with loop antennas for excitation from a Vector Network Analyzer. It then utilizes a particle swarm optimization routine to determine the Debye parameters for a given material within the sample. The system is compared to a common Open-Ended Coaxial Probe technique and found to have similar accuracy for determining the dielectric constant over the same frequency band. This system, however, does not suffer from the same restrictions as the coaxial probe and has a much larger bandwidth than other transmission line methods of similar size.

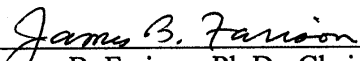
Determining the Complex Permittivity of
Materials with the Waveguide-Cutoff Method

by

Christopher Anderson, B.S.

A Thesis


Approved by the Department of Electrical and Computer Engineering


James B. Farison, Ph.D., Chairperson

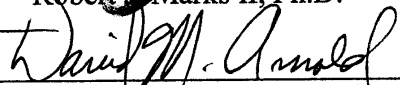
Submitted to the Graduate Faculty of
Baylor University in Partial Fulfillment of the
Requirements for the Degree
of

Master of Science in Electrical and Computer Engineering

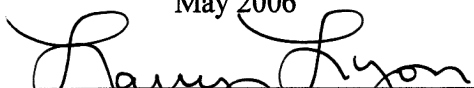
Approved by the Thesis Committee


B. Randall Jean, Ph.D., Chairperson


Robert J. Marks II, Ph.D.


David M. Arnold, Ph.D.

Accepted by the Graduate School
May 2006


J. Larry Lyon, Ph.D., Dean

Copyright © 2005 by Chris Anderson

All rights reserved

TABLE OF CONTENTS

LIST OF FIGURES	iv
LIST OF TABLES	v
ACKNOWLEDGMENTS	vi
CHAPTER ONE: Introduction	1
CHAPTER TWO: Complex Permittivity: Applications and Methods of Measurement	3
Dielectric Characterization	3
Applications of Permittivity Measurement	5
Categories of Dielectrics	7
Methods for Determining the Complex Permittivity	8
CHAPTER THREE: The Waveguide Cutoff Method	22
Introduction	22
Waveguide Transmission Parameter Derivation	23
Calibration Procedure	28
CHAPTER FOUR: Particle Swarm Optimization	31
Introduction	31
Application of PSO to Finding Dielectric Constant	32
Results	44
CHAPTER FIVE: Conclusion	52
APPENDIX A: Getting Started Guide	56
APPENDIX B: Matlab Code	61
BIBLIOGRAPHY	80

LIST OF FIGURES

Figure 1: Diagram of the Waveguide Chamber	25
Figure 2: Cut-plane View of the Waveguide Chamber	26
Figure 3: Waveguide Chamber Cutout	26
Figure 4: Transmission plot of water in the waveguide chamber, X(f), Db vs. Freq. (Hz)	29
Figure 5: Typical Transmission of Air in the Chamber	39
Figure 6: Transmission of 70% Isopropyl Alcohol	40
Figure 7: Air Complex Permittivity	45
Figure 8: Oil Complex Permittivity	45
Figure 9: Acetone Complex Permittivity	46
Figure 10: Ethanol Complex Permittivity	46
Figure 11: Methanol Complex Permittivity	47
Figure 12: Water Complex Permittivity	47
Figure 13: 70% Isopropyl Alcohol Complex Permittivity	48

LIST OF TABLES

Table 1: Constant Values for the Mathematical Model	24
Table 2: Reference for Theoretical Model Training Data	34
Table 3: Static Permittivity Values for Water at 20° C	49
Table 4: Standard Values of ϵ' and ϵ'' at 20° C various Frequencies	49
Table 5: Swarm Calc. Values of ϵ' and ϵ'' for Water at 20 °C at various Frequencies	49
Table 6: Dispersion Parameters for Water (Cole-Cole) at 20° C	49
Table 7: Static Permittivity Values for Methanol at 20° C	50
Table 8: Dispersion Parameters of Methanol (Cole-Cole) at 20° C	50
Table 9: Static Permittivity at DC for Ethanol at 20° C	50
Table 10: Dispersion Parameters for Ethanol (Cole-Cole) at 20° C	50
Table 11: Static Permittivity at DC for Acetone at 20° C	51
Table 12: Dispersion Parameters of Acetone (Cole-Cole) at 20° C	51

ACKNOWLEDGMENTS

I would like to thank my wife Amy, for supporting me through all of my endeavors. I would especially like to thank Dr. Randall Jean for being an excellent mentor, a caring spiritual guide, and a loving friend. Thanks also go to my father, for inspiring me to become an electrical engineer

CHAPTER ONE

Introduction

The measurement of the complex permittivity of liquid and semi-solid materials is an important metrological science. While there are many popular methods for measuring the permittivity of such materials, many of them suffer from complex modeling equations, systematic uncertainties, and high development costs. Most of them also have narrow-band frequency response or require corrections for small systematic errors in the measurement process.

The new method presented in this paper, the Waveguide-Cutoff method, uses a simple mathematical model with a particle swarm curve-fitting algorithm to acquire data. While it could be considered a ‘transmission line’ type of metrology system, it does not suffer from the same frequency restrictions as other waveguide permittivity measurement methods. Most waveguide techniques only utilize the frequency band in the area of the TE₁₀ mode of operation. The Waveguide-Cutoff method, however, utilizes frequencies both below the cutoff frequency as well as those containing additional modes of operation.

This system also has a simple calibration routine and is easy to build. Unlike other systems, the Waveguide-Cutoff method does not suffer from inaccuracies due to sample size and depth. It also has similar accuracy to other methods, having only a 5% margin of error for ϵ_R' and a maximum standard error of ± 3 for ϵ_R'' . Finally, the required hardware does not require very precise machining or special material

modifications, such as silver plating, to produce accurate and valid results. These features make the Waveguide-Cutoff method an excellent addition for determining the complex permittivity of liquids and semi-solids.

CHAPTER TWO

Complex Permittivity: Applications and Methods of Measurement

Dielectric Characterization

The permittivity of a material describes the way in which a material reacts to the presence of an electric field through the storage and dissipation of energy. Any material is electromagnetically characterized by three parameters: its permittivity, ϵ (F/m), its permeability, μ (H/m), and its conductivity, σ (S/m). These parameters may be expressed in constitutive relations for a linear, homogeneous, and isotropic medium:

$$\vec{B} = \mu\vec{H}, \quad (1)$$

$$\vec{J} = \sigma\vec{E}, \quad (2)$$

$$\vec{D} = \epsilon\vec{E} \quad (3)$$

where the magnetic flux density B (Wb/ m²) is related to the strength of the magnetic field H (A/m) by the permeability, the current density J (A/ m²) is related to the strength of the electric field E (V/m) by the conductivity and the electric displacement field D (C/ m²) is related to the electric field by the permittivity.

Homogeneity assumes that these parameters are consistent throughout the material. Linearity assumes that the values do not depend on the relative strengths of the E and H fields. Isotropic refers to the consistency in spatial variations within the material, that is, the values are constant regardless of the orientation of the material. Frequently, these parameters can also depend on temperature, frequency of field excitation, and density.

These three parameters may also be expressed in complex form:

$$\varepsilon = \varepsilon' - j\varepsilon'' \quad (4)$$

$$\mu = \mu' - j\mu'' \quad (5)$$

$$\varepsilon'' = \frac{\sigma}{\omega} \quad (6)$$

where ε' is the absolute dielectric constant, ε'' is the dielectric loss factor, or simply the loss factor in this paper, μ' is the absolute magnetic constant, μ'' is the magnetic loss factor, ω is the radian frequency where $\omega = 2\pi f$, and σ is the conductivity. It is also common to refer to these values in terms of their relation to the permittivity and permeability of free space:

$$\varepsilon = \varepsilon_r \cdot \varepsilon_0 \quad (7)$$

$$\mu = \mu_r \cdot \mu_0 \quad (8)$$

where ε_0 is the permittivity of free space, $8.854187817 \cdot 10^{-12}$. Throughout this paper, the terms permeability and permittivity are considered and discussed in terms of relative form as opposed to absolute form.

Some other important parameters also need to be introduced, as they are also common descriptions for the electromagnetic characterization of materials. The loss tangent, $\tan \delta$, refers to the ratio between the amount of energy lost in a material to the amount of energy stored in a material. Frequently, it is convenient to express a dielectric in terms of its loss tangent as opposed to its loss factor. Explicitly, the loss tangent is related to the values of the dielectric constant and loss factor:

$$\tan \delta = \frac{\varepsilon''}{\varepsilon'} \quad (9)$$

A more extensive description of dielectric parameters has been provided by Geyer in [1].

Applications of Permittivity Measurement

The measurement of dielectric and insulating materials has been studied for nearly as long as the need for the storage of electrical energy. Dielectric materials are essential for modern electronics: from circuit board materials to lumped elements and antenna manufacturing materials. The measurement of these materials has been required for as long as there has been a need to harness electrical energy in a usable form. The scope of this paper will only cover the applications of semi-solids, powders and liquids, for which the Waveguide-Cutoff method has specific application.

In the early 19th century, the principal application of liquid dielectrics was to be used as insulators for transformers and as fillers for high voltage cable according to von Hippel [2]. Several pure liquid dielectrics have been used as reference liquids to test permittivity metrology devices, but recent advances have created a great need for the measurement of not only pure liquids, but of mixtures, colloids, and emulsions as well. Advances in microwave and RF engineering have enhanced the discoveries on the correlation between changes in permittivity and changes in other liquid properties. Changes in temperature, density, viscosity, component composition, quality, and purity may all be quantities that can be related to permittivity for a particular liquid or semi-solid mixture. This wide range of applications has created a large demand for the measurement of permittivity for these types of materials. Two of the largest areas of demand for this type of metrology may be found in industry and in biological applications.

Industrial Applications

Two important industrial applications are composition measurement and process monitoring. Hundreds of processes must be monitored and maintained throughout the manufacturing cycle in order to take raw materials from one form and combine them to create a finished product. Many times, the combination of materials must be monitored to maintain the quality of the product and reduce. By relating the permittivity of the material mixture to the composition of the individual components, it is possible to determine the individual concentrations of each material quickly and efficiently. Extensive research has been done in relating permittivity to different kinds of complex liquids and semisolids. Rung and Fitzgerald describe the effect of permittivity in polymer research [3] and Becher describes its effect in the study of emulsions in [4].

Temperature also has an inverse relation to permittivity and has been used in many process monitoring applications. Chemical processes, food processes and pharmaceutical processes all require intensive time-dependent measurements of temperature, which may be easily accomplished through electric fields without contaminating or reacting with the process itself. One practical application is the monitoring of polymers and thermoplastics. Monitoring the polymer process, either by the amount of catalyst in the reaction or the current temperature of the polymer, is essential in creating a quality product.

Biological Applications

Both the food industry and the biomedical industry have found several applications for the measurement of permittivity. Stuchly noted that different types of tissue have different dielectric properties associated with them [5]. Many parameters in the biological sciences may be related to permittivity, such as the constituent parts of a tissue, the presence or absence of some chemical within tissues and even the presence of cancerous tissue.

The food industry has used microwave permittivity analysis techniques to detect the amount of fat and water content in turkey products as seen in Sipahioglu [6]. The detection and the concentration of water have long been measured using a difference in permittivity due to the innate polarity of the water molecule. For more information about microwave and RF aquametry, see Kraszewski [7].

Other biomedical applications include the measurement of glucose in the bloodstream, such as that reported by Liao[8]. Likewise, cancer cells have a significantly higher relative permittivity than their surrounding tissues, and many attempts have been made to use this fact for non-invasive cancer detection, one of which by Surowiec [9].

Categories of Dielectrics

Dielectrics may be placed into several different categories [1]. These references will be used later for the types of dielectrics that that are applicable to different metrology methods.

Low Dielectric Constant, Low loss ($\epsilon_r' \geq 4, \tan \delta < .001$)

High Dielectric Constant, Low loss ($\epsilon_r' \geq 10, \tan \delta < .001$)

Very High Dielectric Constant, Ultra-Low Loss ($\epsilon_r' \geq 100$, $\tan \delta < .0002$)

Lossy Dielectric ($\tan \delta \geq .1$)

Methods for Determining the Complex Permittivity

There are several methods to measure the dielectric properties of materials at microwave frequencies. An overview of the various types is described by the Agilent Application note [10] and in greater detail by the National Physics Library [12]. The most common types used for liquid and semi-solids are the transmission/reflection method, the open-ended coaxial probe method, the cavity resonator method, and the time-domain spectroscopy method. Each one has features and assumptions that make them distinct for certain applications.

Transmission/ Reflection Method

The Transmission/ Reflection method is used in two major forms: coaxial lines and waveguide structures. These methods utilize the S-parameter scattering matrix to determine information concerning the permittivity and permeability of materials placed within a transmission line. They work well for liquid and semi-solid materials, but solid samples must be precisely machined to fit within the transmission line. Coaxial Line transmission line methods are broadband, having a frequency response from 50 MHz to 20 GHz. This method is excellent for lower dielectric values and error may be around $\pm 1\%$, but higher dielectric measurements may have errors up to $\pm 5\%$ [12]. Since the cavity resonators described later in this section are far superior in determining permittivity for low-loss dielectrics, they should be used instead of transmission line techniques to retain accuracy of measurement.

The waveguide type of transmission line is superior to the coaxial transmission line in that a center conductor is not required when machining samples for the transmission line [12]. Since waveguide transmission line methods are usually only valid in the TE_{10} mode of propagation in the guide, this can restrict the frequency range for waveguide structures down to a decade or an octave in frequency, making them much less broadband than their coaxial line counterparts. The waveguide line sizes for lower frequencies also become large for frequencies below 1 GHz because the lower frequency cutoff of the transmission line is limited by the width of the transmission line. Thus, to produce permittivity measurements at a range of 640 to 960 MHz, a waveguide of 11.5 inches by 5.750 inches would be required. Frequencies lower than this would require large sample sizes and become rather inconvenient.

Permittivity determination process. This method uses a Vector Network Analyzer (VNA) to measure the attenuation and phase shift for the reflection and transmission of the sample. These four values are used to determine the reflection and transmission coefficient for the fields within the waveguide or coaxial line. To accurately relate the resulting S-parameters to these coefficients, the exact dimensions of the sample and the total transmission length must be known. These equations are derived and solved explicitly in the NIST standard: “Transmission / Reflection and Short-Circuit Line Permittivity Measurements” by Baker-Jarvis [13]. Once the transmission and reflection coefficients for transverse waves entering and exiting the sample have been determined, they can then be related to the complex permittivity and permeability of the sample. This method assumes that no surface currents exist on the normal surface of the sample, or the surface which is normal to z-direction. It further

assumes that the wave in the sample is either transmitted or reflected, but not dissipated in the form of surface currents.

Measurement process. A precisely machined sample is placed within the coaxial line or waveguide, so that the outer dimensions of the sample closely match the inner dimensions of the guiding medium. This placement prevents small leakages and reflections from occurring on the waveguide walls. The surface orthogonal to the direction of transmission must also be machined to be exceedingly flat and perfectly orthogonal to the direction of propagation. The VNA then excites the transmission line and both the phase change and attenuation are recorded at each frequency. Now that the S-parameters are known, they can be related to the permittivity through the transmission and reflection coefficients.

Transmission line methods are effective at frequencies where the length of the sample is not a multiple of one half wavelength in the material. In normally constant dielectric materials, this original method produced large spikes in the real part of permittivity at these resonant frequencies within the sample. A much better mathematical solution for finding the permittivity may be found in [13]. It involves using an iterative procedure to correct for the resonant frequencies that naturally occur when relating the permittivity to the S-parameters. One useful relation may be found in equation 7:

$$\frac{1}{2} \{[S_{12} + S_{21}] + \beta[S_{11} + S_{22}]\} = \frac{z(1 - \Gamma^2) + \beta\Gamma(1 - z^2)}{1 - z^2\Gamma^2} \quad (7)$$

where β is a correction parameter based upon the loss of the sample, z is the transmission coefficient and Γ is the reflection coefficient. The solution found by

Baker-Jarvis uses the Nicholson-Ross-Weir equations as a starting value and the Newton-Raphson root finding technique to iteratively solve for the permittivity. Now that errors in the numerical relations have been resolved, it is important to note other uncertainties that must be corrected in the permittivity measurement.

Accuracy and Sensitivity Analysis. There are several sources of error that can happen in this particular method of permittivity calculation. Small gaps between the sample and the sample holder and uncertainty in the exact sample length can lead to large errors in the actual calculations of the permittivity. In coaxial structures, the error is significantly increased due to air gaps around the center conductor, since the electric field is strongest at that point in the transmission line.

It is possible to correct for air gaps through several means. Some authors have compensated for the problem of sample air gaps by treating the coaxial line as a layered frequency independent capacitor by Westphal in [14], and Bussey in [15], [16]. The resulting equation for the real part of permittivity is similar to a first order Debye model and is shown below:

$$\varepsilon_R'(f) = \varepsilon'_{R\infty} + \frac{(\varepsilon'_{Rs} - \varepsilon'_{R\infty})}{1 + (\omega)^2 \cdot \tau^2} - j \frac{j\omega\tau \cdot (\varepsilon'_{Rs} - \varepsilon'_{R\infty})}{1 + (\omega)^2 \cdot \tau^2} \quad (8)$$

where ε'_{Rs} is the relative permittivity at DC, $\varepsilon'_{R\infty}$ are and the relative permittivity at infinity, and ω is the angular frequency. This equation shows that the relaxation time depends upon both the relative permittivity as well as a DC conductivity value.

Uncertainty in the position of the reference plane positions can also lead to large error in the calculation of the phase parameter [12]. Normally, samples are placed in exact positions within the guiding structure, with known distances from the transmitting

the receiving antennas. When the samples are slightly misplaced from these positions, these errors in the reference plane positions will occur. This occurs due to errors in the calculation of the reflection coefficients from the S-parameters received from the VNA.

Coupling to higher order modes within the guide can also lead to error measurements in the waveguide structures. This can occur if a material of unknown dielectric constant lowers the frequency instance of the higher order modes. This will only occur with very high dielectrics and software can easily be used to compensate for these problems.

Cavity Perturbation Method

The Cavity Perturbation Method has several benefits over other forms of permittivity measurement. It is the most accurate method for measuring very low-loss dielectrics. Unlike the coaxial probe technique, there is no calibration to perform or maintain to acquire valid measurements. Not as much material is required in the measurement process as compared to other methods, although the samples do require very specific machining to fit in the cavity. While some cavity perturbation techniques have been created to be broadband by Raveendranath [17], most of them will find the dielectric constant and the conductivity at either one single frequency, or at a narrow band of frequencies.

Dielectric cavity resonators come in several different shapes and sizes. Most take the form of rectangular and cylindrical waveguides, where the positions of the maximum E and H fields are easily determinable. Different sample shapes may be used within the chamber, but the equations that govern the final relation between the complex permittivity, resonant frequency and Q-factor must be derived for each sample

shape. Some common types of sample shapes are rods and spheres, which have simple, predictable geometries when solving for the fields within the sample.

One problem with this particular method is that it is single band in nature. It is possible to achieve some band variance by changing the physical dimensions of the cavity to move the unperturbed resonant frequency. A micrometer is used to determine the change in length of the resonator, which in turn is used to determine the effective Q-factor.

Permittivity Determination Process. The original frequency resonance and effective Q of the cavity must first be determined when the cavity is empty. Once the sample is inserted, the shift in frequency as well as the change in Q is noted. Q is defined as the ratio of the energy stored in the cavity to the amount of energy lost per cycle in the walls due to conductivity. The method assumes that the change in the overall geometrical configuration of the resultant fields from the introduction of the sample into the cavity is effectively zero. When the sample is added to the chamber, there is a change in the resonant frequency of the chamber as well as a decrease in the Q factor. These two changes can be directly related to the dielectric constant and the conductivity of the sample.

Measurement Process. The cavity is excited at two ends through small irises with a VNA. First, the empty chamber is excited to find the resonant frequency and empty chamber Q factor. Then, the sample is inserted through small holes in the sides of the chamber and excited again. If the fields for the cavity can be explicitly determined, then these two parameters can be used to calculate the conductivity and the

ϵ_r' of the sample material. The derivations for the actual calculation of the conductivity and real part of permittivity by Chao may be found in [18].

There is a tradeoff to note in the practical determination of the Q-factor. This value can be roughly determined from the 3-dB point method as described in [12]. This simple calculation requires the user to find the 3-dB power point of the resonance and measures the width of the peak at that point. The width of the resonance at this point is directly related to the Q-factor of the cavity. A more complex and complete calculation is the S-Parameter method for determining the Q-factor of the resonating chamber. This method corrects for the error of leakage at any point in the detection system of the guide and can be used to automatically determine the Q-factor through means of a curve-fitting algorithm. The tradeoff here is that the 3-dB power point method is simple and easy to perform, but can be erroneous if the Q of the cavity is too small. Thus, only larger cavities with unperturbed Q-factors should utilize this technique. Resonators in the RF and microwave band typically have unloaded Q-factors on the order of 10^2 to 10^6 [12], and resonators with Q-factors as low as the 100s may be used effectively with decent results. The automatic technique, however, requires a non-linear curve fitting regression and significant amount of programming and calibration in order to be successful.

Some simple modifications may be made to this process for different types of materials. For measuring permittivity, the sample should be placed in the position of the peak electric field. This ensures that both the fields within the sample will be uniform and that there will be a measurable change in Q-factor, since most of the energy within the cavity will be dissipated from a change in electric field. For

measuring permeability, it is best to place the sample in the peak magnetic field position, so that most of the energy dissipated will be through surface currents within the sample. This creates the largest change possible in Q-factor losses due to permeability, and provides much more accurate results in the final calculation of this parameter as described by Waldron in his principal work on cavity perturbation [19].

Accuracy and Sensitivity Analysis. The dielectric perturbation method has several assumptions that affect the quality of the resulting values of ϵ_R' . First, the sample is assumed to be homogeneous and isotropic. The size of the sample must also be small in proportion to the resonator used. A sample that is too small causes too small a change in the Q factor and in frequency. This reduces the SNR of the instrument, as the absolute error is large as compared to the change in Q and $\Delta\omega$. Ideally, the sample must be small enough for the fields in the cavity to be uniformly large in terms of the sphere, however, a sample that is too large may not satisfy the assumptions made for the perturbation approximation. Smaller samples are usually used to reduce the error in the actual perturbation approximation [17]. The physical size of the resonator itself is also a factor to consider for determining the ideal sample type. While large resonators provide a much higher unperturbed Q-factor, a resonator that is too large may also reduce the overall effectiveness of the measurement.

Two other sources of error for this method include resonant leakages and the introduction of other modes within the cavity. Any kind of connector interface may cause a non-resonant coupling between the input and output port, thus decreasing the overall energy storage of the instrument. When the perturbation theory is used in long-

rod type resonators, it is possible to introduce other modes than simply the TE_{10} into the cavity, which greatly affects the resulting amplitude of the resonant frequency.

The absolute error of the cavity perturbation technique was found to be 5% for rod-type sample Cavity Perturbation systems by Carter [20].

Coaxial Probes

The Open-ended coaxial probe method was first introduced by Stuchly et al. [21]. Since their inception, extensive research has been done to improve the performance of these devices for their shortfalls. The device usually consists of a VNA, a length of coaxial cable, connectors and an open (sometimes flanged) coaxial end.

There are many reasons for the widespread use of the coaxial probe technique. The system is broadband and effective for liquids and semi-solids. The coaxial probe is a simple structure compared to other forms of permittivity measurement and has a straightforward model to derive the dielectric constant. The system is also non-destructive, and does not require the modification of the material under test (MUT) as other systems require.

There are some restrictions in the use of coaxial probes. Many coaxial probes cannot accurately describe the characteristics of very low loss materials, i.e. $\tan \delta < 0.05$. The probes themselves are also susceptible to error with changes of temperature after calibration. While some inaccuracies in some of the assumptions can be corrected using calibration kits, calibrations for certain conditions must be performed frequently to ensure measurement accuracy. Some specific types have been used in high temperature situations by Gershon [22].

Measurement Process. Once the probe has reached temperature equilibrium within the environment, the calibration is performed by taking open and shorted measurements. The probe is then placed in a material with known dielectric properties, such as water or saline at a known temperature. The material should be at least half as wide as the maximum width of the probe itself, and the sample thickness should allow for the magnitude of the electric field should be two orders of magnitude smaller than that of the strength at the probe/MUT interface. The system assumes that the MUT is homogeneous and isotropic. The surface of the MUT should also be as clean and as flat as possible, to avoid the error in an air cavity between the surface of the material. Because the fringing fields from the end of the probe have such a large affect on the final calculation of the reflection coefficient, air gaps can create large errors in the final calculation of the permittivity [12]. Some systems have been created to compensate for this [14], but some commercial versions by Agilent do not [10] [23]. Another cause of error is the loss of calibration by changing the temperature of the substance, or simply by perturbing the length of cable between the VNA and the coaxial line. These errors may be reduced with the purchase of an automatic calibration kit supplied by the manufacturer [23].

Permittivity Determination Method. A TEM wave travels down the length of the coaxial wire from the VNA and creates a “fringe” of an electrical field inside the MUT. This field changes shape as it enters the material from the coaxial line, and produces a certain reflection (Γ) and a change in phase θ . The relationship between the reflection coefficient and the phase change cannot be explicitly related to the complex permittivity, however, and must be optimized. One interpolation routine has involved

utilizing tables of the Γ for a specific frequency, ϵ_R' and $\tan \delta$. The intersection point between the contours of the reflection coefficient and the phase response would then be mapped to specific values of ϵ_r' and $\tan \delta$ [21].

Accuracy and Sensitivity Analysis. For the unrestricted range of operation, that is when the loss tangent is greater than 0.05, the absolute error for current commercial coaxial probe techniques is around 5% of ϵ_R' . The degree of accuracy in this technique is limited by errors in measurement and in modeling. Measurement errors occur from the roughness of the sample surface and unknown sample thickness as described by ChunPing et al [24]. Modeling errors can occur from imperfections in the short-circuit plane and neglecting the higher order modes that may exist in the coaxial cable [12]. In general, the sensitivity of the instrument depends on the value of the loss tangent. The smaller the value of the loss tangent, the less sensitive the coaxial line method becomes. It is important to ensure proper calibration while testing and to remove any air-gaps between the end of the probe and the sample while performing measurements. These are the largest causes for uncertainty in the measurement process and can account for up to an error of 400% or more.

Time-Domain Spectroscopy

Time-Domain Spectroscopy has several advantages over the other frequency-based techniques mentioned earlier. With an instrument working in the time-domain, one single measurement covers a very wide frequency range, sometimes up to two decades [25]. This technique works not only in the microwave range, but also into the lower frequency RF range as well. This method does particularly well with low

dielectric constant, high DC conductivity materials. It can perform rather high in frequency, but the upper bandwidth limit depends entirely on the sampling speed of the instruments. One problem with this technique is its hardware dependence and low noise tolerance. Any noise on the line can distort the output when the information is brought into the frequency band via an FFT. Since most of the information is acquired after this transformation, any additions of noise or jitter to the signal before translation can have a drastic effect on the calculations of the dielectric constant.

This method includes several parts to make up the instrument: high frequency sampling oscilloscope, a picosecond pulse generator with rise times around 35-45ps, signal averagers with AD converters, and data acquisition systems to process the data.

Measurement Process. For this technique, the sample is placed at the end of a coaxial transmission line that has been terminated with a short. Then, a chirp-pulse or step-pulse is produced by a pulse generator, which propagates through a coaxial line, entering the sample. The pulse reflects off of the shorted end of the line, passing back through the transmission line and is received at an exact point in time by the high frequency oscilloscope. The difference between the original time domain signal and the reflected signal acquired at the input describes the electromagnetic properties of the MUT.

Permittivity Determination Method. A step-like pulse is produce in the time domain by a pulse generator and propagates down the transmission line. This transmission line has a very accurately measured length, so that the calculation of the permittivity may be accurately calculated. This pulse then passes through the material,

is reflected by a short circuit and passes through the material again. The difference in time from the pulse creation and receiving the reflected pulse contains the dielectric properties of the sample [25]. Since the travel time for the transmission line with and without the sample is known, the resulting FFT of the pulse and the transmission time difference

Accuracy and Sensitivity Analysis. Accuracy for this particular method depends almost exclusively on the quality of the time-domain instrumentation, sampling frequency, and noise threshold. Averaging of time-domain signals must be performed, since a single sweep may have large noise content. The accuracy seems to decrease at higher frequencies. In [25], the accuracy of the TDR system for measuring the permittivity of methanol was “distorted” above 25 GHz. At this frequency, the sampling rate of the instrument began to degrade the accuracy of the system. Within the available frequency band, from 100KHz to 25GHz, the error of the system was only a few percent.

Other Methods

Other methods exist for finding the permittivity of materials, but will not be extensively explained, due to their low frequency application and specialization for only hard-solid dielectric materials.

Parallel Plate. The parallel plate method for finding the dielectric constant is simple. The machined sample is placed between two electrodes, whose ends are connected to a Capacitance meter or RLC Analyzer, and the resultant capacitance of the material is calculated. Using this value and the dimensions of the sample between the

electrodes, the permittivity over a range of frequencies may be determined. Since the highest frequency for most RLC Analyzers is around 3 GHz, this instrument is effective at lower frequencies, but not high enough to be compared to the other methods [13].

CHAPTER THREE

The Waveguide Cutoff Method

Introduction

An alternative solution for finding the permittivity of powdered solids and fluids has been found. For this system, a small rectangular chamber is filled with dielectric material. The S-parameters of the transmission through the chamber, or S_{21} , are recorded using a Vector Network Analyzer. The results are then fed into an optimization routine that fits a model to the real data from the VNA. From this fitted model, the values of complex permittivity may be calculated.

One phenomenon that has been utilized to determine the dielectric constant of materials is the cutoff frequency in a rectangular chamber. As a transmission line, a waveguide structure has an operational frequency band with an upper and lower frequency limit. Waves are transmitted most efficiently in the dominant mode, which is TE_{10} for a rectangular waveguide. The upper frequency limit for transmission is usually the frequency for which the width of the waveguide is large enough to allow the propagation of the first non-dominant mode. That is, the width of the waveguide must be small enough to only allow the excitation of dominant mode for the chosen frequency of transmission. The lower frequency limit, called the cutoff, refers to the inability for lower frequency waves to propagate down the transmission line. This phenomenon is due to the wavelength being longer than the width of the waveguide.

The following equation shows the low frequency cutoff for an ideal rectangular waveguide:

$$f_c = \frac{1}{2\pi\sqrt{\mu\varepsilon}} \sqrt{\left(\frac{m\pi}{a}\right)^2 + \left(\frac{n\pi}{b}\right)^2} \quad (10)$$

where f_c is the cutoff frequency in Hertz, a is the width of the waveguide in meters, b is the height of the waveguide in meters, m is the number of $\frac{1}{2}$ -wavelength variations of fields in the "a" direction, n is number of $\frac{1}{2}$ -wavelength variations of fields in the "b" direction, μ is the permeability of the material inside the waveguide, and ε is the complex permittivity of the material inside of the waveguide

If the permeability of the material is assumed to be equal to that of vacuum, the cutoff frequency is simply a function of the permittivity of the material within the waveguide.

In [26], this phenomenon was applied to calibrate microwave sensors in industrial applications by Jean. The S-parameters and the cutoff frequency were used to determine various physical properties, such as the water and fat content in meats, the amount of dye and water in pulp stock, and the amount of water in some microwave food products. This particular instrument, however, uses the same information to find the complex permittivity in a more general form.

Waveguide Transmission Parameter Derivation

To accurately determine the permittivity of the material in the chamber, we must first derive the mathematics for the model of an ideal waveguide, and then determine the parameters that must be calibrated or experimentally determined to create a model of the imperfect waveguide. The waveguide used for this system has a

transmission length of four inches and a width of 1.875 inches. The guide has been fashioned from aluminum for ease of construction and is held together with bolts.

Waves are launched into the chamber by two loop antennas placed in the center position of the chamber, at either end of the waveguide. They are excited from two SMA type high frequency connectors that connect directly to the Vector Network Analyzer. The loop antennas are held behind a water-tight seal made of Ultem, isolating them from the material, and terminated in a 50 Ohm load. The placement of the excitation antennas in the center of the guide prevents the detection of certain modes in the resulting transmission parameter signal. The constant values required thus far are the transmission length of the rectangular waveguide, the width between the metallic plates, the permittivity and the permeability of free space. Table 1 shows these values.

Table 1: Constant Values for the Mathematical Model

Parameter	Value	Units
Length of Chamber, L	.047625	meters
Width of Chamber, a	.1016	meters
Permeability of Free space, μ_0	$4 \cdot \pi \cdot 10^{-7}$	
Permittivity of Free Space, ϵ_0	$8.854187817 \cdot 10^{-12}$	

One useful model for the characterization of complex permittivity is the Debye relaxation model. This model has the following parameters: the conductivity, σ , the relaxation time, τ , the initial relative permittivity or the permittivity at DC, ϵ_i , and the final relative permittivity, ϵ_f , which is the permittivity at infinite frequency. The following equations govern a first-order Debye model:

$$\epsilon_p(f) = \epsilon_f + \frac{(\epsilon_i - \epsilon_f)}{1 + (2 \cdot \pi \cdot f)^2 \cdot \tau^2} \quad (11)$$

$$\varepsilon_{pp}(f) = \frac{(\varepsilon_i - \varepsilon_f) \cdot 2 \cdot \pi \cdot f \cdot \tau}{1 + (2 \cdot \pi \cdot f)^2 \cdot \tau^2} + \frac{\sigma}{2 \cdot \pi \cdot f \cdot \varepsilon_0} \quad (12)$$

A diagram of the waveguide can be found in Figure 1.

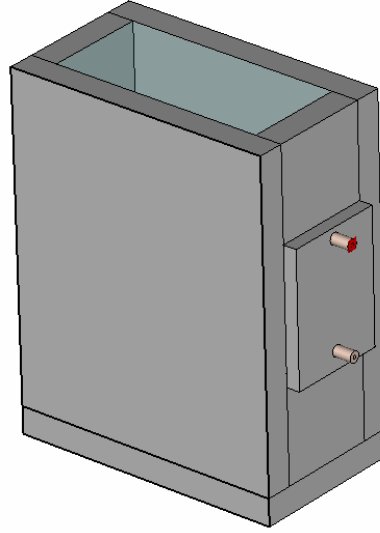


Figure 1: Diagram of the Waveguide Chamber

Figures 2 and 3 show a more descriptive cut-plane version of the antenna loop feed structures and the inside of the chamber. The two loop antennas send a wave down the length of the waveguide in the z -direction. For a rectangular waveguide, the k vector for propagation in the z direction is

$$k_z^2 = (2 \cdot \pi \cdot f)^2 \cdot \mu \cdot \varepsilon - \frac{(m \cdot \pi)^2}{a} - \frac{(n \cdot \pi)^2}{b} \quad (13)$$

where k_z is the propagation vector, m is the mode number denoting the number of half cycle variations of the fields in the direction of length a , or the x -direction. The variable n is the mode number denoting the number of half cycle variations of the fields in the direction of length b or the y -direction. The width and height of the waveguide are a

and b . μ is the permeability of free space, and $\epsilon = \epsilon_0 (\epsilon' - j \epsilon'')$, the complex permittivity of the material within the waveguide.

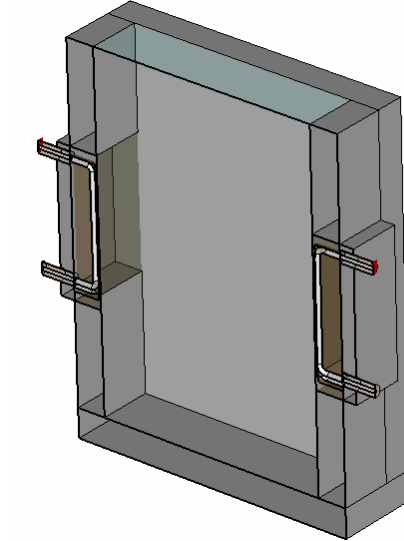


Figure 2: 3D Cut-plane View of the Waveguide Chamber

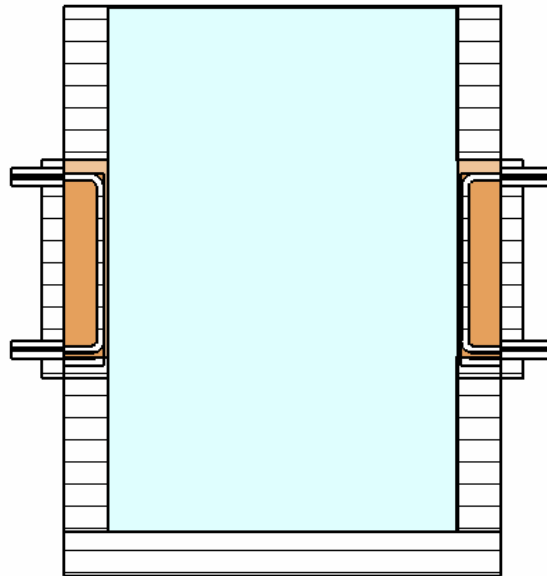


Figure 3: Waveguide Chamber Cutout

If the complex permittivity equations, (11) and (12) are combined with equation (13), and the propagation vector k_z is isolated, the following equation is produced.

$$k_z(f, m) = \sqrt{(2 \cdot \pi \cdot f)^2 \cdot \mu_0 \cdot \varepsilon_0 \cdot \varepsilon'(f) - \frac{(m \cdot \pi)^2}{a^2} - j \cdot (2 \cdot \pi \cdot f)^2 \cdot \mu_0 \cdot \varepsilon_0 \cdot \varepsilon''(f)} \quad (14)$$

The complex transmission of a wave is represented in polar form by the following equation:

$$S_{12}(f, m) = e^{-j \cdot K_z(f) \cdot z} \quad (15)$$

where k_z is the propagation vector, m is the mode and z is the position in the waveguide where the receiver has been situated. The vector network analyzer will output the total transmission through the waveguide, which must be accounted for by using the mode dependent equation for transmission, equation (15).

$$S_{12}(f, m) = e^{-j \cdot K_z(f, m) \cdot z} \quad (16)$$

After plugging in the value of L , the length of the chamber at the position of the receiving antenna, our equation finally becomes:

$$S_{12}(f, m) = e^{-j \cdot K_z(f, m) \cdot L} \quad (17)$$

For each mode, m , that can exist within the guide over the frequency range of interest, a corresponding term must be included in the model for the total additive transmission. By adding all of the modes together, the logarithmic ratio between the energy excited by the transmitting antenna and the energy received by the other antenna may be represented (in Nepers).

$$X(f) = \ln(S_{12}(f, 1) - S_{12}(f, 2) + S_{12}(f, 3) - S_{12}(f, 4) + S_{12}(f, 5) - S_{12}(f, 6) + S_{12}(f, 7)) \quad (18)$$

The even modes are then subtracted from the total transmission. While the presence of the even modes within the waveguide is not seen by the receiving antenna, their existence still removes energy from what will be received.

To account for the output of the VNA, which produces transmission parameters in decibels, the total transmission was scaled by a value of 8.686 to translate from Nepers into dB.

$$X(f) = 8.686 \left[\ln \left[\frac{(e^{-j \cdot K_z(f,1) \cdot L} + e^{-j \cdot K_z(f,3) \cdot L} + e^{-j \cdot K_z(f,5) \cdot L} + e^{-j \cdot K_z(f,7) \cdot L})}{-e^{-j \cdot K_z(f,2) \cdot L} - e^{-j \cdot K_z(f,4) \cdot L} - e^{-j \cdot K_z(f,6) \cdot L}} \right] \right] \quad (19)$$

This equation governs the transmission S-parameters over the frequency range of interest for an ideal waveguide. As stated earlier, however, this model must be calibrated for the idealized model to accurately represent the actual transmission of an actual waveguide.

Calibration Procedure

The first problem to solve in creating an accurate model for this rectangular chamber was to ensure that the magnitude of the modeled transmission and the real transmission contained the same features at the same frequencies. When equation (19) from above was evaluated using the standard Debye parameters for water, and the values compared to the actual transmission of water in the chamber, quite a bit of error was noted. Figure 4 shows a comparison between the two plots of $X(f)$.

To attempt to rectify the difference, scaling factors were added to equation (19); the new equation is noted in equation (20). One single scaling coefficient was not sufficient for correcting the attenuation offset between the mathematical model and the

actual transmission, since each of the modes could be contributing different amounts of energy.

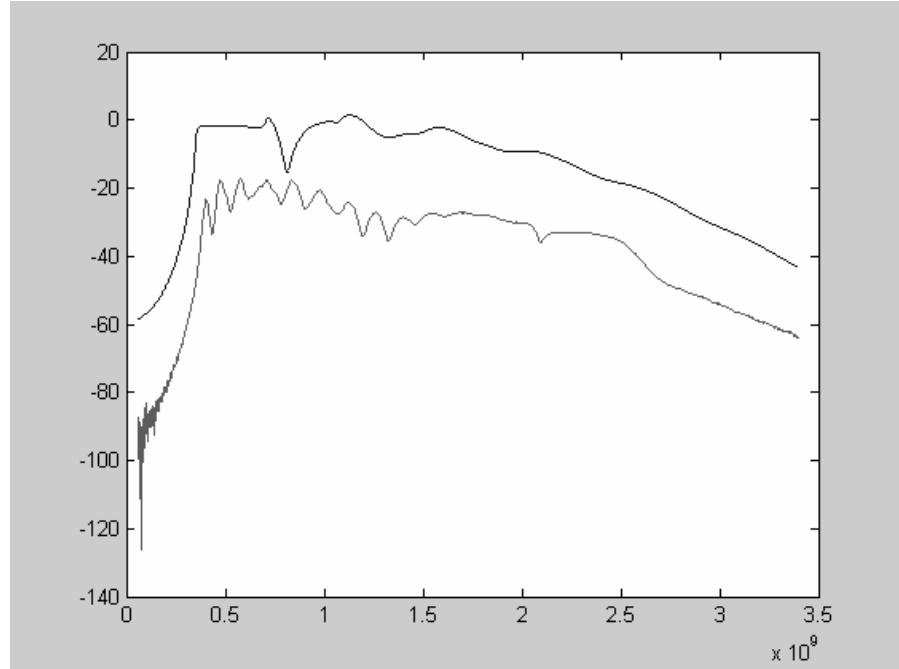


Figure 4: Transmission plot of water in the waveguide chamber, $X(f)_{\text{Db}}$ vs. Frequency (Hz)

Therefore, a scaling coefficient was added for each of the modes in the mathematical model. In this fashion, both the difference in attenuation as well as the energy contribution for each of the modes in the total transmission could be accounted for.

$$X(f) = 8.686 \left[\ln \left[\begin{array}{l} (c_1 e^{-j \cdot K_z(f,1) \cdot L} + c_2 e^{-j \cdot K_z(f,3) \cdot L} + c_3 e^{-j \cdot K_z(f,5) \cdot L} + c_4 e^{-j \cdot K_z(f,7) \cdot L}) \\ -c_5 e^{-j \cdot K_z(f,2) \cdot L} - c_6 e^{-j \cdot K_z(f,4) \cdot L} - c_7 e^{-j \cdot K_z(f,6) \cdot L} \end{array} \right] \right] \quad (20)$$

The constants, c_1 through c_7 , are called the mode coefficients. To empirically determine these values for the chamber, dielectric materials with known model parameters were placed within the chamber. These model parameters were then applied to the mathematical model to produce a theoretical transmission plot. This theoretical plot was then compared to an actual plot for the transmission of that particular material by

least squared error. The mode coefficients were determined from a particle swarm optimization that minimized the error between the theoretical model and the actual transmission through the guide. The reference materials used were water, ethanol, air and isopropyl alcohol.

Another set of parameters required for the calibration were the electrical dimensions of the chamber. Impurities in the waveguide walls, rough spots and residues from the machining process, thermal expansion from temperature differences, and a score of other unknown effects could affect the effective electrical dimensions of the chamber. These dimensions appear as the width, a , the length, L , and the height b , and are used in the propagation vector calculation, k_z . Since these values change due to humidity and temperature, a calibration routine was constructed to find their values at the exact time of measurement. Variations in these values can produce significant changes in the final calculation of the permittivity. A variation of even .0001 cm in the waveguide length caused the ϵ_R' to change from 79.5 to 80.5 when water was placed in the chamber. For this reason, it is important that these values are calibrated before taking any actual measurements. By placing known substances in the waveguide, such as air and water, and reporting the current temperature of the water, these values can be quickly calculated.

CHAPTER FOUR

Particle Swarm Optimization

Introduction

In the previous chapters, many of the specific steps for finding the mode coefficients and the electrical chamber dimensions were not explained. This section will describe specific methods and techniques for producing these values. A non-linear least squares search algorithm is used in conjunction with the calibrated transmission of the chamber to produce the Debye model parameters for the material within the chamber.

Particle Swarm Optimization (PSO) is a population-based optimization routine using stochastic solution placement. It was originally inspired by the social behaviors among flocking birds and schooling fish by Eberhardt and Kennedy [27]. PSO begins by randomly guessing a series of solutions across an n-dimensional space, where n is the number of parameters to be optimized. Each of these solutions is considered a single particle. At specified time intervals, the error for the solution of every particle is calculated, and the solution with the smallest error is saved as each particle's personal best. If the error for a particle is less than the current error of the global best solution, the solution of that particle replaced the global best solution. After the errors are calculated, the particle moves in a new direction and velocity, which depend both on the calculated personal best solution as

well as the global best solution. Over time, the particles will reach the global best and the optimization routine will report the current global best as the final solution.

In this particular application, a PSO is used to fit the modeled curve of the S_{21} transmission coefficient to the actual curve from the VNA. The model is modified by changing the values of the four Debye parameters, ϵ_f , ϵ_i , σ , and τ . By changing these four parameters, the PSO can minimize the error between the modeled S_{21} plot and the actual S_{21} plot. When the error is at a minimum, it can be assumed that those four Debye parameters will describe the dielectric properties of the material within the waveguide chamber.

Application of PSO to finding Dielectric Constant

The PSO algorithm is also used for determining the mode coefficients as described in Chapter 2, as well as the Debye model parameters for the material under test (MUT). The mode coefficients are the constant values that scale the additive effects of each of the modes for the total $X(f)$ or transmission parameters.

Recall from chapter two that while the transmission through the waveguide can be modeled effectively, there is an error due to the unknown contribution of each of the modes within the waveguide. A PSO was used to find coefficients for each of the modes to match the theoretical model to the real data. To find these parameters, the mathematical model from chapter two was used in a fitness function for a PSO. It was assumed that these coefficients were only dependent on the electrical properties of the waveguide structure itself. It was hoped and successfully proven that these values did not depend on the dielectric material within the waveguide and only on the waveguide itself. Four different references were used simultaneously to calculate the error value

for each particle. The mode parameters for each particle were used to calculate the total transmission for each of the four materials. The resulting transmission was used to calculate the error for that material, and the errors for each of the four material curves were added together to produce the total error. Four materials were used to ensure that the PSO found mode coefficients that worked for a wide range of materials in predicting permittivity, and not simply one particular type of material. In this fashion, all of the error contributions were accounted for by finding these coefficients and matching the modeled data to actual data from the guide.

Four sets of training data were used to find these mode parameters. The transmission parameter plots for air at 25°C, distilled water at 25°C, ethanol at 25°C and 70 % isopropyl alcohol at 25°C were used as references for the mathematical model. These substances were chosen for of their known dielectric model values as well as their wide range of value. Air and water are the references used in the Open Ended Coaxial Line Dielectric Probe kit, which have well known model parameters and were readily available as calibration materials.

Training Data Acquisition

The dielectric constant measurements used in all of the swarm training were determined using an Agilent Open-Coaxial line 85070E Dielectric Probe Kit with a Hewlett Packard 8720ET Vector Network Analyzer. This system is a broadband metrological tool that determines the dielectric constant of materials over a frequency range from 200MHz to 20GHz. The values from this kit were used in determining the mathematical model parameters for the isopropyl alcohol solution. According to the datasheet, the dielectric probe kit has an absolute accuracy for measuring dielectric

constant of $\pm 5\%$. The value of ϵ_R' of air used in the calibration routine was a constant 1.0008. A first order Debye model was used for the water, ethanol and isopropyl alcohol with the following parameters:

Table 2: Reference for Theoretical Model Training Data

Parameter	Water	Ethanol	Isopropyl Alcohol, 70%
Final Permittivity, ϵ_f	4.9	4.5	2.6811
Initial Permittivity, ϵ_i	78.982	24.7	31.27
Relaxation time, τ	8.309×10^{-12}	$1.7637e^{-10}$	$3.9378e^{-11}$
Conductivity, σ	1000×10^{-5}	$3.1e^{-4}$.015311

Complete Swarm Explanation

The swarm begins by randomly scattering ‘particles’ across the solution space as possible solutions. The particles initially assume a known set of model parameters and then are moved to random areas about that initial solution by adding a random value to each of the model parameters. A fitness function named `mode_fitness()` is called, which outputs the total mean-squared error between the mathematical model and the data from the VNA. The software begins by calculating the curve fit for each of the particles using the `mode_fitness()` function and choosing the solution with the smallest error as the global best. Then, velocities of a given direction and step width are applied to each particle. Each iteration moves the particles according to the following update equations:

$$v[] = v[] + c1 * \text{rand}() * (\text{pbest}[] - \text{present}[]) + c2 * \text{rand}() * (\text{gbest}[] - \text{present}[]) \quad (21)$$

$$\text{present}[] = \text{present}[] + v[] \quad (22)$$

Where $v[]$ is the current velocity, $present[]$ is the current position, $rand()$ is a random number between 0 and 1, $gbest[]$ is the global best position, $pbest[]$ is the personal best position of the particle and $c1$ and $c2$ are constant learning parameters.

The velocity update equation takes the previous velocity and adds values according to the pull from both the personal best of that particle as well as the global best for the system. This means that the particles are pulled both toward the best value that they have found and the best value that all the particles have found. Given enough iterations, nearly all the particles will find their way to the global best solution. For each particle, the current position is used to calculate this error, and the software compares the current position to the local best and the global best. If the error for the current position is less, then the current values will replace the local best or global best values respectively.

For the mode swarm, ten particles were allowed to wander for 400 time steps before declaring the seven final mode coefficients. For the Debye swarm, ten particles were allowed to swarm. For further instruction on the use of the `debye_swarm()` matlab functions, see Appendix A.

Learning Parameters and Swarm Tradeoffs

The learning parameters used in the `mode_swarm()` and the `debye_swarm()` are $c_1 = 0.1$ and $c_2 = 0.05$. These values were chosen after trying out several different configurations, and they seemed to scale well with the magnitude of the values for the swarm. If the value of the swarm variable has an order of magnitude of 1, it would be imprudent to give the update equation a step size of 10 or 100. The particles could simply skip over the actual global best value. Again, choosing learning parameters that

are very small requires the swarm to run a large number of iterations before it actually finds the global best position.

In designing a swarm, there are tradeoffs between total processing time, output variance, and the number of particles used in the optimization. If only a small number of particles are used in the swarm, there is less chance that one of them will find the global minimum value for the optimization. More particles means more of them to find the minimum and pull the others toward the global best position in the optimization. This translates to a smaller variance between different passes through the swarm, but also means a much larger amount of memory required to run the optimization. The personal best matrix, pb , is of size m by n , where m is the number of optimization parameters and n is the number of particles. With multi-dimensional spaces, large amounts of memory can be required to store these matrices and perform the mathematics on them. The number of iterations can also affect the computation time. The longer the swarm is allowed to run, the more accurate the final answer will be, since the particles will come closer to the actual global minimum; however, more iterations means longer processing time, sometimes with negligible increases in accuracy.

Noise Injection

A well documented problem for particle swarm optimization is the concept of falling into false minima. Frequently, a particle will exactly hit a false minimum value and pull the rest of the particles toward it, away from the global minimum. This problem is combated by the utilization of noise injection, or swarm explosion. A discussion of this type of phenomena may be found in [28]. The swarm will allow the

particles to roam for a time, and then send all of them in a random direction at a very high velocity, usually an order of magnitude higher than the normal frequency for the particles in the swarm. The global best stays the same, however, and will still affect the particles once they have been given the freedom to roam normally. This gives the particles a second chance on finding the global minimum and help to prevent them from focusing on local minima in the solution space. The `debye_swarm()` function utilizes two noise injections after both 100 iterations and 300 iterations.

Dielectric Constant Particle Swarm Optimization

After finding the mode coefficients, the values were then used to determine the Debye values for the complex permittivity over the frequency range of interest. The seven mode coefficients found for the previous swarm in the test data were then used as constant values in a program called `Debye_swarm()`. This program accepted the data from the S-parameter plot from the VNA and would output the four values of a Debye model: the final ϵ' value, ϵ_f , the initial ϵ value, ϵ_i , the relaxation time, τ , and the conductivity, σ . From the addition of the calibrated mode coefficients, the mathematical model accurately fits the actual output data from the VNA.

Electrical Length Calibration

With only compensating for the mode coefficients, there was still a slight amplitude offset in the negative direction for every plot that was calculated by the swarm. To compensate for this, two of the model values and constants were perturbed slightly. It was found that when the length and width of the chamber were changed even by .01 cm, the amplitude of the complex permittivity changed significantly. The

difference in electrical length versus physical length can be explained by the active region of the loop antennas. A wave is not created in the waveguide cavity until the established fields are in the far-field region of the antenna. Since this region is unknown in this configuration, it was necessary to compensate for this unknown length. A second calibration swarm, similar to the mode swarm, was created to find the effective values for the electric lengths of the transmission length and the width of the waveguide.

Data Preparation

Signal pre-processing for the transmission through the waveguide was required for the swarm to perform its role successfully and efficiently. The transmission of energy through the chamber has a similar form regardless of the dielectric MUT. In every case, there is a sharp increase at the front end, representing the low-frequency cutoff of the waveguide for the given material. This is followed by a flat or slowly decreasing region, where the transmission of frequencies is fairly constant. After this, there is a larger decreasing region, where the higher order modes have begun to attenuate the signal of high frequency waves within the waveguide. A graph of the transmission of air within the chamber may be found in Figure 5.

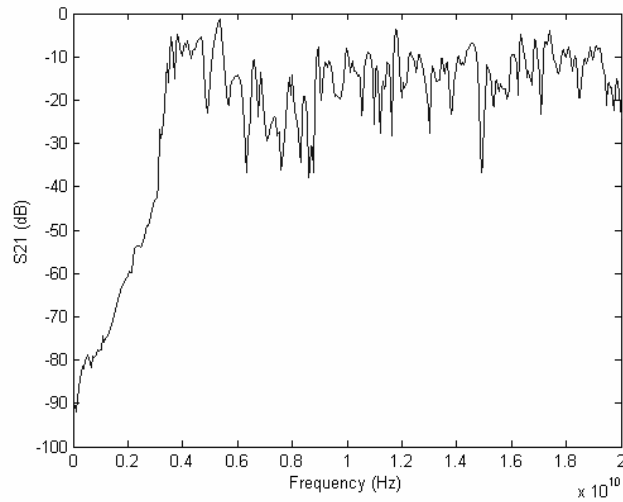


Figure 5: Typical Transmission of Air in the Chamber

These three regions can have various lengths over a wide range of frequencies. Notice that the final region for the transmission of air through the chamber is not represented, because the VNA used only had a maximum bandwidth of 20 GHz. Other materials, such as alcohols, have a rather narrow-band frequency response. An example can be found in the transmission of 70% isopropyl alcohol in figure 6. For isopropyl alcohol, all three regions have been represented in over a range of only 3GHz. This wide variability between substances led to several problems for the particle swarm. One problem stemmed from the noise floor of the VNA. Take note of the average value for the transmission of the Isopropyl alcohol from figure 6.

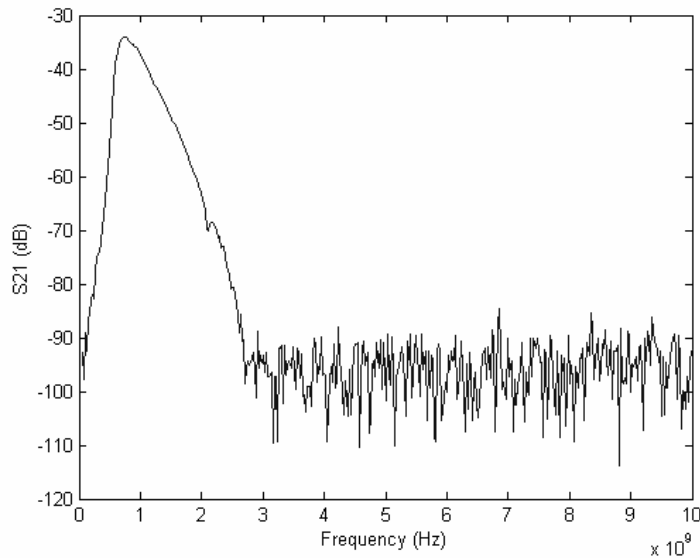


Figure 6: Transmission of 70% Isopropyl Alcohol

Most of the value of the transmission is below the noise floor of the instrument, which is about -90 dB in this case. Using a graph such as this, the swarm would not only try to fit a curve according to the acceptable transmission data from 50 Mhz to 3Ghz, but also try to include the noise data section from 3 Ghz to 10 Ghz. This would create large errors in the final parameter determination, since the swarm would simply fit a straight line along the noise region and ignore the smaller region of valid data. This was easily fixed with a noise floor removal. Before the swarm is called, any data that contains values below -70 dB is removed, leaving only valid transmission data for the swarm to work on.

Another problem stemmed from the starting point of the particle swarm. Originally, the particles were only given one starting point: the Debye parameters for water. This was found to be inadequate when performing the swarm on dielectrics with high attenuation, such as ethanol, methanol, and isopropyl alcohol. Even after running

for long periods of time, the swarm would produce answers far greater than that of the normal parameters for these materials.

Since several of the test materials had graphs similar to isopropyl, a simple test was created to use two different starting points. If the average value of the transmission through the chamber was greater than -50, it was assumed that the transmission plot was similar to water, and used those Debye parameters as a starting point. If the average value was less than -50, the swarm assumed the starting point to be a greatly attenuated dielectric similar to ethanol.

Statistical Analysis

With an accurate model, valid data being passed into the swarm, and a variable starting point to deal with different types of dielectrics, the swarm was complete. To produce actual plots for the dielectric of materials however, some statistical analysis was required for the swarm to reliably produce the same answer every time for a given dielectric. Recall the discussion of the tradeoff between the length of processing time for the swarm and the variance of the values that the swarm produced. The global best solution for the curve fit in the Debye swarm is not the same each time the swarm has completed the designated number of iterations. To produce a final global best, the swarm is run several times, and the average values for each of those global bests are calculated. A function, `iterative_debye_swarm()`, has been created to run a swarm for a designated number of times and perform the required statistical analysis on the resulting swarms. The software first creates an n by 5 matrix of global best solutions by running the swarm n times. The function then tests for outliers within the Debye parameters. This process first involves calculating the median for the ϵ_i parameter.

This parameter effectively controls the y-intercept point of the graph. Any small deviations in the initial permittivity can cause a vertical shift in the graph and a very large overall error. Once the median has been determined the function removes any answers that are not within one standard deviation from the median. It is common for one in 15 trials of the PSO to be far from the actual global best. This phenomenon can be explained by the fact that other local minimums exist in the solutions space in addition to the global minimum. Sometimes the particles report these local minimums as global minimums, and produce a global best that is far from what most other iterations have produced. With the addition of the statistical analysis, the error for the system is reduced to a level consistent with other methods of dielectric measurement techniques.

After the first removal of outliers, the process is repeated two more times using the mean value of the ϵ_i parameter. This process removes smaller variations between iterations: usually global best values that are 5-7 points higher or lower than the mean global best. The Debye parameters that are left are then re-assembled into matrices using the original Debye model. For each of these, the average value at each frequency is produced. The output for the complex permittivity over the total range of frequencies comprises these two matrices of averaged values, ϵ' and ϵ'' .

One thing to consider with the output of the ϵ' and ϵ'' is that they are interpolated at the high frequencies. Recall that only values that will enter the swarm from the transmission S_{21} VNA data are the portions of the graph that reside above the instrument noise floor. In many cases, this can restrict the frequencies for which the Debye parameters can be reliably calculated. In the case of the

iterative_debye_swarm() function, the reported values for ϵ' and ϵ'' have been extrapolated at the higher frequencies, however, extrapolation cannot occur at the lower frequencies in all cases. While the iterative Debye swarm will produce values of ϵ' and ϵ'' which are accurate at the frequencies under test, the ϵ_i that is produced may not actually represent the value at DC, but instead the ϵ_i at the minimum frequency of the sample. The results section provides a more explicit example of this phenomenon.

Uncertainty Analysis

An expansive uncertainty analysis was not a requirement for this particular instrument. There are two types of uncertainty: random uncertainty and systematic uncertainty. Systematic uncertainty refers to any bias or offset inherent within the instrument. Random uncertainty is refers to any uncertainty from random factors and noise. Random uncertainty may be corrected by taking several different values repeatedly and averaging them, while systematic error must be corrected by offsets. The Waveguide-Cutoff method refers to a calibration routine for translating the transmission S-parameters into dielectric constant through a curve-fitting routine. There are no moving parts or physical measurements required, and since the nature of the system is a calibration to remove offset, there are no systematic errors to report. Most analyses of this type refer specifically to the systematic errors, but since there are no systematic errors inherent to the system above and beyond that of other methods, no extensive explanation shall be given. One systematic error in almost all methods of permittivity measurement is the uncertainty of the Vector Network Analyzer. For the results below, the uncertainty plots may be found in the literature for the HP 8720ET [29]. PSO is a type of stochastic search algorithm and will naturally have a random

process associated with it. Several different corrections are made to reduce the random error associated with the search algorithm, including noise injection, statistical analyses to remove outliers as well as iterative averaging for the final Debye parameters. The software also reports the standard deviation of the initial permittivity measurement, so that the user can quickly determine whether or not the final model parameters are accurate.

Results

The following Figures contain typical results for the `iterative_debye_swarm()` function as compared to the Agilent Open Coaxial Line Dielectric Probe Kit. In all cases, the dielectric probe kit is the solid line and the PSO is represented by a dotted line. Following these figures are the numerical results from the Waveguide cutoff method system as well as reference data for each material. The reference data tables contain information from various sources and data in various forms. While broadband dispersion data was preferred, this was not always available, and comparisons were made to whatever data could be found for each material. The error calculations in the tables were calculated from the mean-squared error between the reference data and the results from the test system.

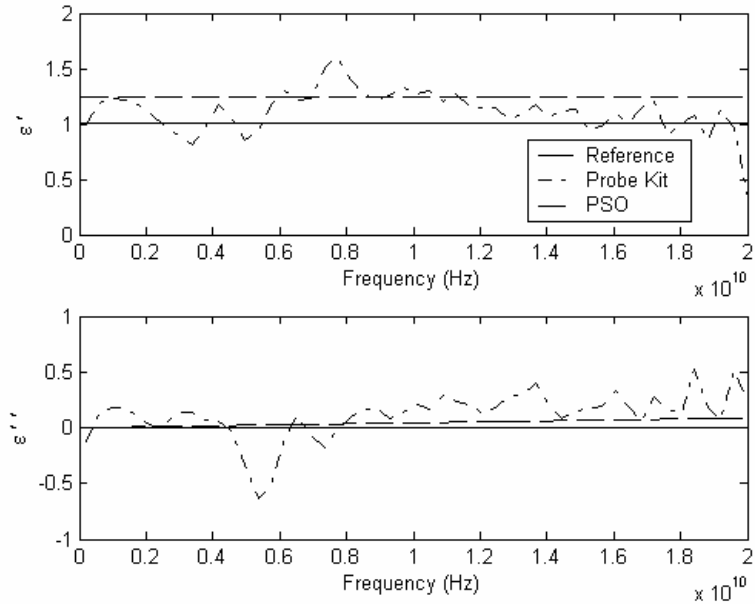


Figure 7: Air Complex Permittivity

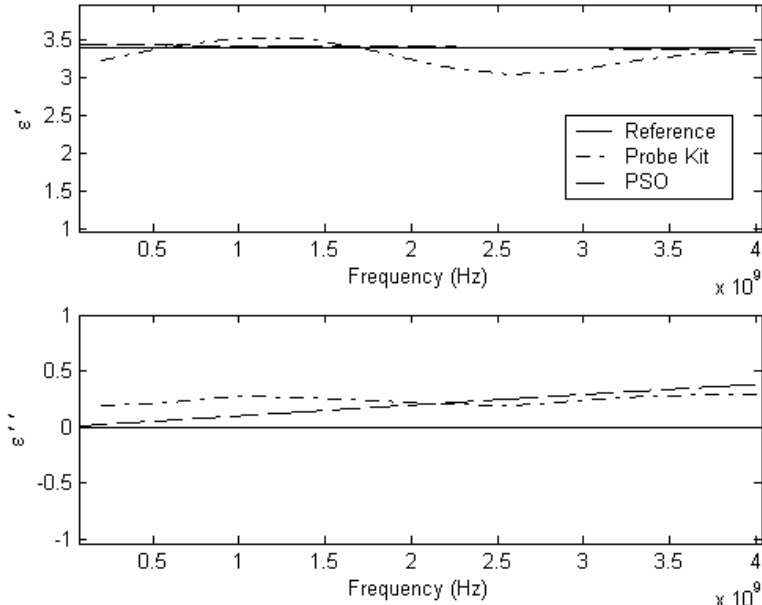


Figure 8: Oil Complex Permittivity

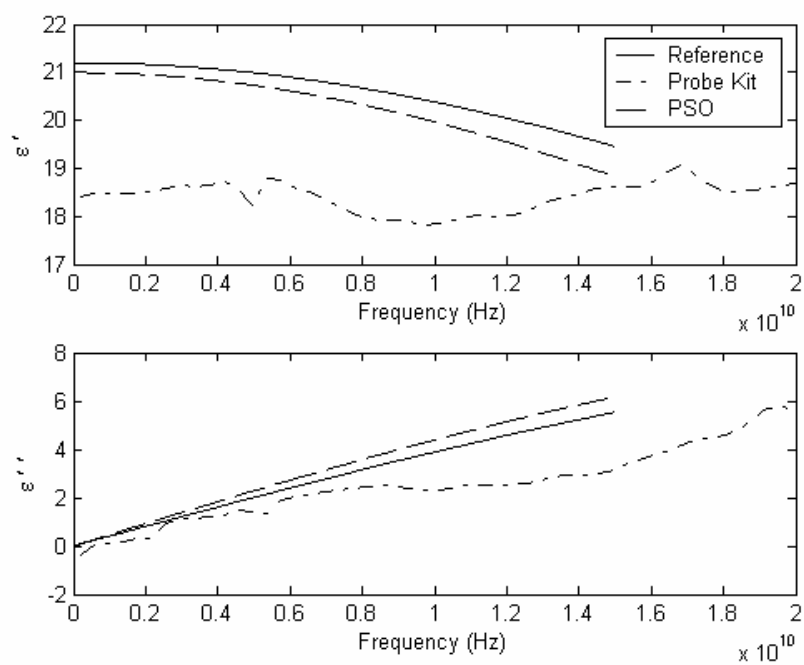


Figure 9: Acetone Complex Permittivity

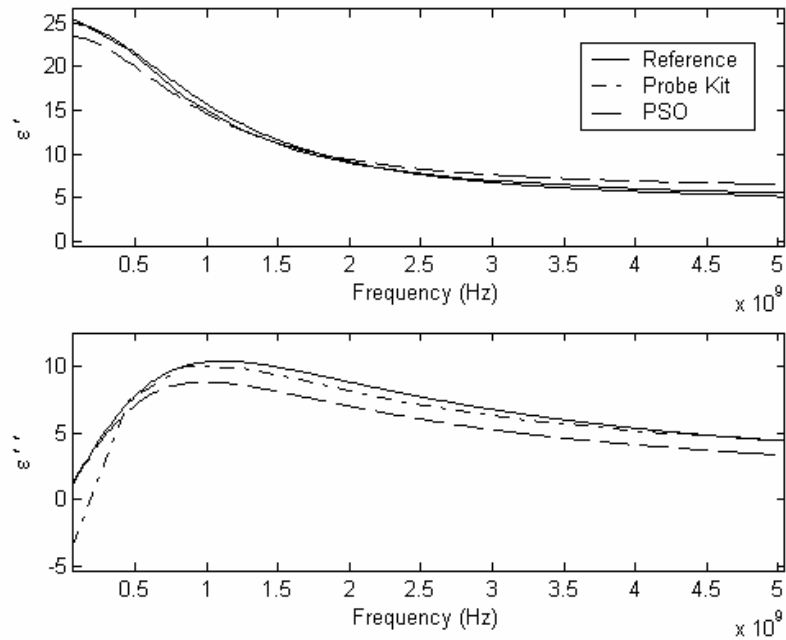


Figure 10: Ethanol Complex Permittivity

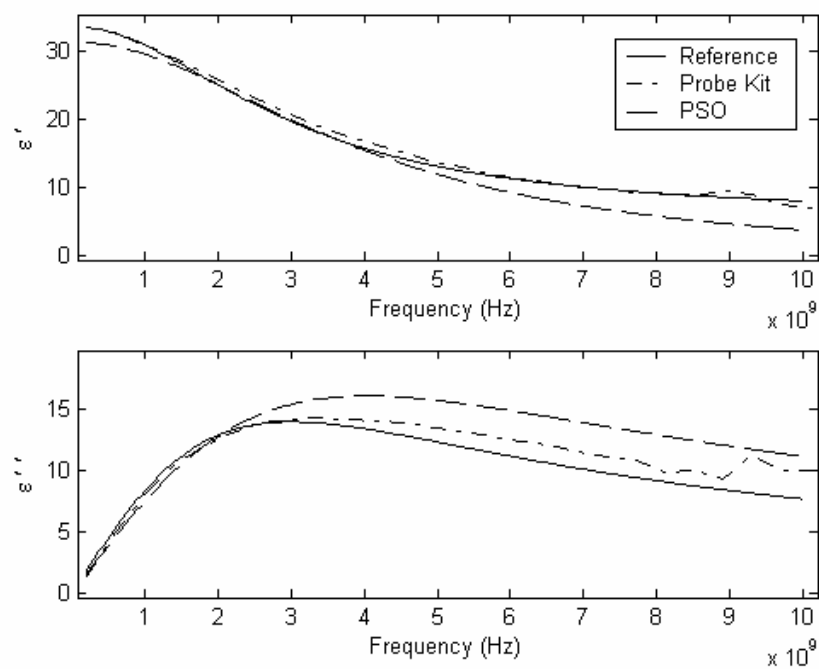


Figure 11: Methanol Complex Permittivity

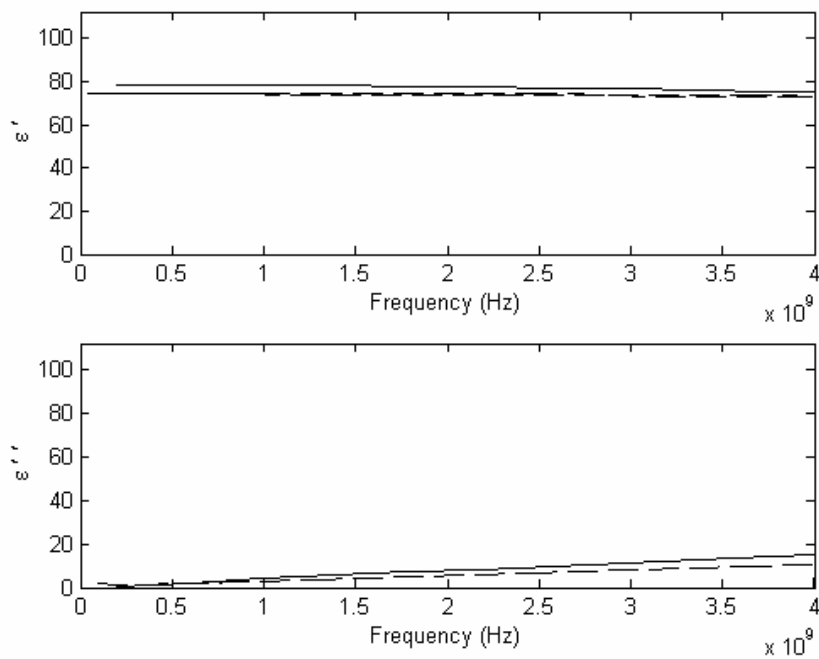


Figure 12: Water Complex Permittivity

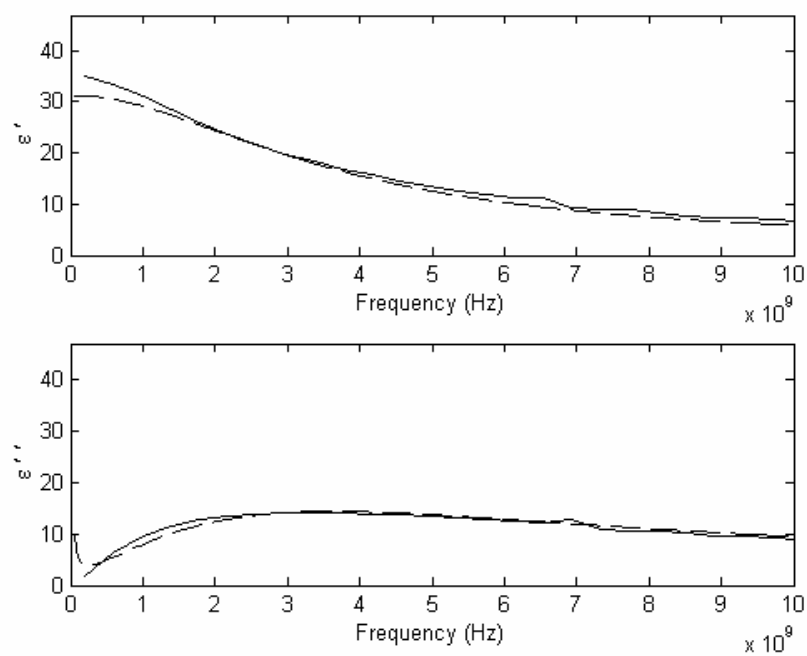


Figure 13: 70% Isopropyl Alcohol Complex Permittivity

Water

Swarm Calculated value of $\epsilon_i = 74.93$

Table 3: Static Permittivity Values for Water at 20 °C

ϵ_i at 1 Mhz (20 °C)	\pm	Source
80.27	.11	Gregory and Clarke [30]
80.21	.5	Kaatze et al [31]

Table 4: Standard Values of ϵ' and ϵ'' at at 20 °C various Frequencies [32]

Frequency	Permittivity (ϵ') at 25°C	Loss Factor (ϵ'') at 25°C
1 MHz	78.36	0
10 MHz	78.36	0.04
100 MHz	78.36	0.38
200 MHz	78.35	0.76
500 MHz	78.31	1.90
1 GHz	78.16	3.79
2 GHz	77.58	7.52
3 GHz	76.62	11.13
4 GHz	75.33	14.58
5 GHz	73.73	17.81
10 GHz	62.81	29.93
20 GHz	40.37	36.55

Table 5: Swarm Calculated Values of ϵ' and ϵ'' for Water at 20 °C at various Frequencies

Frequency	Permittivity (ϵ') at 20°C	Loss Factor (ϵ'') at 20°C
1 GHz	74.80	2.95
2 GHz	74.51	5.43
3 GHz	74.01	7.99
4 GHz	73.34	10.50

Table 6: Dispersion Parameters for Water(Cole-Cole) at 20 °C [33]

ϵ_f	ϵ_i	α	λ_c (cm)	ϵ' Error	ϵ'' Error	Source
5.2	80.4	0	1.78	3.92%	19.65%	[33]

Methanol

Swarm Calculated value of $\epsilon_i = 31.287$

Table 7: Static Permittivity Values for Methanol at 20 °C

ϵ_i at 1 Mhz (20 °C)	\pm	Source
33.64	.06	Gregory and Clarke [30]
35.70	.03	Kienitz and Marsh [34]
34.8	.5	Jordan et al [35]
33.65	.1	NPL 1990 [31]
32.62	.03	Cunningham [36]
32.65	.1	NPL 1990 [31]
31.70	.1	NPL 1990 [31]
29.86	.05	Kienitz and Marsh [34]

Table 8: Dispersion Parameters (Cole-Cole) at 20 °C

ϵ_f	ϵ_i	α	λ_c (cm)	ϵ' Error	ϵ'' Error	Source
5.7	33.64	0	10	3.32 %	12.34 %	[33]

Ethanol

Swarm Calculated value of $\epsilon_i = 25.3393$

Table 9: Static Permittivity at DC for Ethanol at 20 °C

ϵ_i at 1 Mhz (20 °C)	\pm	Source
25.16	.04	Gregory and Clarke [30]

Table 10: Dispersion Parameters for Ethanol (Cole-Cole) at 20 °C

ϵ_f	ϵ_i	α	λ_c (cm)	ϵ' Error	ϵ'' Error	Source
4.2	25.07	0	27	5.16 %	14.48 %	[33]

Acetone

Swarm Calculated value of $\epsilon_i = 21.08$

Table 11: Static Permittivity at DC for Acetone at 20 °C

ϵ_i at 1 Mhz (20 °C)	\pm	Source
21.13	.04	Gregory and Clarke [30]
21.01		Lide [37]

Table 12: Dispersion Parameters for Acetone (Cole-Cole) at 20 °C

ϵ_f	ϵ_i	α	λ_c (cm)	ϵ' Error	ϵ'' Error	Source
1.9	21.2	0	.63	4.96%	1.69 %	[33]

Soybean Oil

Swarm Calculated value of $\epsilon_R' = 3.41$

Accepted values of $\epsilon_R' = 3.1$ at 30 MHz

The ϵ_R' for soybean oil at 20 °C is about 3.4 [38]

Air

Constant $\epsilon' = 1.0005$

Calculated Swarm $\epsilon' = 1.28$

CHAPTER FIVE

Conclusions

From the results, the produced system has proven to be at least as accurate as the Open Coaxial-Line Dielectric Probe kit. The datasheet on the probe kit claims that the typical accuracy for the instrument is $\pm 5\%$ of the $|\epsilon_R^*|$. For the Waveguide-Cutoff system, only the value of air does not fall within this 5% tolerance range. This is reasonable, however, since the probe kit's standard deviation for the dielectric of air also falls outside of the 5% range. Because of this error, it can be concluded that the 5% accuracy should only be applied to materials with a DC permittivity of greater than two. In some cases, the accuracy of the Waveguide-Cutoff method produced a value much better than the probe kit, as in the case of acetone.

Not only is the system accurate, but it does not require any precise machining, since any error associated in the machining process is removed by the calibration routine. The system presented here was created with simple materials and did not require special transmission line enhancements in order to produce valid results. No silver plating was added to the inside of the guide, and the sides were created from aluminum and Ultem.

Like the open coaxial line dielectric probe kit, this instrument utilizes a wide spectrum, and could be modified to work at different frequency ranges. With smaller or larger waveguide chambers, both frequency bands smaller and wider than the 20GHz bandwidth represented for this particular system could be achieved. For any rectangular

chamber with similar construction and excitation, the mathematical model could still be applied.

The system also uses a simple mathematical model and a singular curve-fit in order to produce valid data. The introduction of particle swarm optimization to find the values of dielectric constant is also a fairly new idea. Several papers have been written on applying particles swarm optimizations to solve several complicated problems in the field of electromagnetics [39]-[42], but not specifically to finding the complex permittivity of materials. Curve fitting, parameter prediction, filter design, and antenna design are complex problems that have been solved successfully using optimization routines such as the ones used here. This method for finding the dielectric constant is simple to emulate, requires little coding, and is effective once it has been calibrated. The software written here could very easily modified for use on a smaller or larger sized chamber, with minimal changes to the code. While a particle swarm curve-fitting algorithm is used for this specific solution, any non-linear least squares algorithm could be applied to the mathematical model for optimization and produce valid results. The PSO used in this system is a unique feature that could be utilized in other permittivity measurement systems to improve performance.

The calibration of the instrument is simple in comparison to the dielectric probe kit. For this instrument, the Vector Network Analyzer needs to have a ‘through’ calibration performed before the connectors are attached to the chamber. After the one-time calibration to find the unknown parameters mentioned in the previous chapters, the user need only perform the VNA calibration as needed, and should not require a re-derivation of the mode constants and electrical length constants very often. Once the

instrument has been connected for the first time, the mode parameters for the chamber and the electrical dimensions of the waveguide will need to be determined with the methods mentioned in Appendix A. This section provides explicit instructions on how to use the Matlab functions to perform the one-time calibration.

The system does not, however, suffer from the same systematic errors of measurement that the Open Coaxial-line probe kit has. When measuring low-loss liquids, the depth of the sample plays a crucial role in the accuracy of the instrument. If the penetration depth is greater than the depth of the sample, then a large reflection may occur off of the bottom of the container, producing a very large error in the measurement. The probe kit also suffers from air bubbles beneath the probe when placed within the sample. Such bubbles can create large errors and should be removed to produce valid results. The Waveguide-Cutoff method is a much easier method to use when measuring the permittivity of liquids than the Open Coaxial-line probe kit.

Other than uncertainty, it has a much wider frequency bandwidth than other methods mentioned in the above chapters. Most other waveguide transmission line methods have only a decade or an octave of frequencies. Variable-size cavity resonators as well as most Time-Domain spectroscopers also have a frequency band of only a couple of decades at most.

APPENDICES

APPENDIX A

Getting Started Guide using the Debye Parameter Particle Swarm Functions

Waveguide Parameter Setup

In this section, the parameters for the waveguide, the mode parameters and the electrical length parameters shall be determined. This step requires the use of a Vector Network Analyzer (VNA), several dielectric reference materials, and the waveguide cavity for calibration. It will be assumed in this section that the user understands the use of the VNA and can operate it successfully. Running these Matlab functions does not require the use of any functions not found in the standard toolbox. No extra toolboxes are required. The software was created on Matlab v. 6.1, but it should work on newer versions. All data that is passed into these functions is assumed to be column data. That is, frequency and transmission are separate columns, as opposed to rows.

Determining the Mode Coefficients

Begin by setting your Matlab directory to the Mode_Swarm_Mod folder. All the functions you will need for this part of the setup will be in this file folder. Determine the S_{21} parameters for several different reference materials for your waveguide cavity. Most VNAs have the ability to save waveforms onto disks, through the serial port or through a GPIB bus. Once you have this data, use the 'import' command in Matlab to create a matrix whose first column is frequency data, and the second column is the S_{21} parameter data. Make sure that your VNA has been set in the logarithmic scale for the y-axis for transmission data, since the model assumes that it is

received data in units dB. It is suggested that the user should only choose reference materials that have known Debye or constant permittivity parameters. The `mode_fitness()` function uses a dielectric model, chosen by the user, to simultaneously fit a transmission parameter curve for a particular material. The user should try to use the materials already selected within the `mode_fitness()` function inside the `Mode_Swarm_Mod` folder. These four substances, water at 25 °C, Air at 25 °C, Isopropyl alcohol at 25 °C, and ethanol at 25 °C, all have known parameters for dielectric, and the dielectric models have already been simulated in the fitness function. To use a different reference material, the four Debye parameters must be known and changed in the `mode_fitness()` function. **Make sure to change the waveguide dimensions in all fitness functions for every function that has been run.** These values are called 'a' and 'L', and must be changed if a different sized waveguide is used from the one used here. Once all four reference have been taken, the following function call can be made in matlab.

```
>>mode_coefficients = mode_swarm(test1, test2, test3, test4)
```

In the default case, test1 is the water reference, test2 is the isopropyl alcohol reference, test3 is the air reference and test4 is the ethanol reference. Remember that all four tests should be 2 by n, where n is the number of data points taken in the transmission sample from the VNA. This test should take about 5-15 minutes depending on the processing speed of your computer. The user should run this several times and produce many different `mode_coefficients` before choosing one set. What may work for one set of

materials may not work for any material placed in the guide. It took several runs for the writer to produce a valid and reliable set of mode coefficients.

Once this has completed and the mode coefficients are known, the electrical length parameters will now be determined. The required m-files are in the Dimension Calibration folder. This swarm utilizes the calibrated mode coefficients from the previous section and attempts to refine the model even further by swarming the two dimensions of the waveguide, the width and the length. This swarm is slightly more refined than the last one. Due to the drastic changes of dielectric constant with a small change in the waveguide dimensions, the step size for this swarm has been significantly reduced. The function call is similar to the mode coefficient swarm.

```
>> dimensions = cal_swarm(mode_coeff, test1, dielectric_ref)
```

where `mode_coeff` is the vector created from the previous section, `test1` is water at 25 °C, and `dielectric_ref` is a matrix providing the dielectric constant and loss factor of water at 25 °C. If valid data cannot be attained from another source, such a matrix can be created from the `debye_plot()` m-file in the rectangular swarm folder. This is simply a function that accepts the four debye model parameters and produces vectors for ϵ' and ϵ'' . The function call is seen below:

```
>>permittivity_matrix = debye_plot(Debye, test1)
```

where Debye is the set of four parameters that make up the model and test1 is a vector or matrix of frequency values for which the user would like the Debye model calculated. Any data from a rectangular waveguide matrix will work here, since the function only utilizes the frequencies. Just as before, the user may want to run the cal_swarm function to find the dimensions several times to make sure that the values will accurately fit real data.

With all of the parameters determined, all values are available for use in the final function to determine the dielectric constant of the material within the waveguide cavity. The function to actually run the swarm a number of times and perform statistical analyses to determine the final permittivity of the substance may be found in 'Rectangular Swarm\Explosion_model'. The complete function call may be seen below.

```
>> [t_ep, t_epp, debye] = iterative_debye_swarm(test_rect, test_dielectric, Coeff3,
numruns, conductivity)
```

t_ep and t_epp are vectors of the ϵ' and ϵ'' values for the swarm. The debye variable is the matrix of determined Debye parameters that the final plot is based upon. The test_rect variable is the S_{21} data from the VNA for the material under test. The test_dielectric variable is a reference vector that will be compared to the material within the waveguide. The conductivity value must be a value of '1' or '0'. This tells the swarm whether or not to include the conductivity parameter in the swarm. For non-conductive materials, this parameter should be set to '0'. For conductive materials, the

value should be set to '1'. Any substance may be used to compare to the MUT. Coeff3 is the mode coefficients found from the mode_swarm call. The numruns variable determines how many iterations the function will run, or how many times the final swarm values will be calculated. Usually a value of 10-15 is adequate to produce an accurate value for permittivity.

APPENDIX B

Matlab Code

Mode_Fitness

```
function error = mode_fitness(constants, test1, test2,
test3, test4, flag)
% test one is water, test 2 is Isopropyl alcohol, test 3
is Air, test 4 is ethanol

f1=test1(:,1)';

% parallel plate dimensions in inches
a = 1.875;
L = 4;

sizefreq1 = length(f1);
e0 = 8.854187817e-12;
u0 = 4*pi*1e-7;
a = a*.0254;
L = L*.0254;

% begin Water
con = 1000e-5; % in Siemens/meter
ei = 78.982;
efv = 4.9*ones(1,sizefreq1);
ef= 4.9;
tau = 8.309e-12;

ep1 = efv + (ei-ef)./(1+(2*pi*f1).^2*tau^2);

part1 = ((ei-ef)*2*pi*tau.*f1);
part2 = (1+(2*pi*f1).^2*tau^2);
part3 = con./(2*pi*f1*e0);
eppl = part1./part2 + part3;
Kz = [ ];
for m = 1:7

part1 = (2*pi*f1).^2*u0*e0.*ep1;
part2 = ((m*pi)^2)/a^2*ones(1,sizefreq1);
part3 = j*(2*pi*f1).^2*u0*e0.*eppl;
```

```

temp= sqrt(part1-part2-part3);
Kz = [Kz; temp];
end

imp1 = exp(-j*Kz(1,:)*L);
imp2 = exp(-j*Kz(2,:)*L);
imp3 = exp(-j*Kz(3,:)*L);
imp4 = exp(-j*Kz(4,:)*L);
imp5 = exp(-j*Kz(5,:)*L);
imp6 = exp(-j*Kz(6,:)*L);
imp7 = exp(-j*Kz(7,:)*L);

Calc1 = 8.686*log(abs(constants(1)*imp1 +
constants(2)*imp3 + constants(3)*imp5 + constants(4)*imp7
- constants(5)*imp2- constants(6)*imp4-
constants(7)*imp6));

% begin Isopropyl
f2=test2(:,1)';
sizefreq2 = length(f2);
con = .015311;
ei = 31.27;
efv = 2.6811*ones(1,sizefreq2);
ef= 2.6811;
tau = 3.9378e-11;

ep2 = efv + (ei-ef)./(1+(2*pi*f2).^2*tau^2);

part1 = ((ei-ef)*2*pi*tau.*f2);
part2 = (1+(2*pi*f2).^2*tau^2);
part3 = con./(2*pi*f2*e0);
epp2 = part1./part2 + part3;
Kz = [ ];
for m = 1:7

part1 = (2*pi*f2).^2*u0*e0.*ep2;
part2 = ((m*pi)^2)/a^2*ones(1,sizefreq2);
part3 = j*(2*pi*f2).^2*u0*e0.*epp2;

temp= sqrt(part1-part2-part3);
Kz = [Kz; temp];
end

imp1 = exp(-j*Kz(1,:)*L);
imp2 = exp(-j*Kz(2,:)*L);
imp3 = exp(-j*Kz(3,:)*L);
imp4 = exp(-j*Kz(4,:)*L);

```

```

imp5 = exp(-j*Kz(5,:)*L);
imp6 = exp(-j*Kz(6,:)*L);
imp7 = exp(-j*Kz(7,:)*L);

Calc2 = 8.686*log(abs(constants(1)*imp1 +
constants(2)*imp3 + constants(3)*imp5 + constants(4)*imp7
- constants(5)*imp2- constants(6)*imp4-
constants(7)*imp6));

% begin Air
f3=test3(:,1)';
sizefreq3 = length(f3);
ep3 = 1*ones(1,sizefreq3);

epp3 = 1*ones(1,sizefreq3);
Kz = [ ];
for m = 1:7

part1 = (2*pi*f3).^2*u0*e0.*ep3;
part2 = ((m*pi)^2)/a^2*ones(1,sizefreq3);
part3 = j*(2*pi*f3).^2*u0*e0.*epp3;

temp= sqrt(part1-part2-part3);
Kz = [Kz; temp];
end

imp1 = exp(-j*Kz(1,:)*L);
imp2 = exp(-j*Kz(2,:)*L);
imp3 = exp(-j*Kz(3,:)*L);
imp4 = exp(-j*Kz(4,:)*L);
imp5 = exp(-j*Kz(5,:)*L);
imp6 = exp(-j*Kz(6,:)*L);
imp7 = exp(-j*Kz(7,:)*L);

Calc3 = 8.686*log(abs(constants(1)*imp1 +
constants(2)*imp3 + constants(3)*imp5 + constants(4)*imp7
- constants(5)*imp2- constants(6)*imp4-
constants(7)*imp6));

% begin ethanol
f4=test4(:,1)';
sizefreq4 = length(f4);
con = 3.1e-4;
ei = 24.7;
efv = 4.5*ones(1,sizefreq4);

```



```

ef= 4.5;
tau = 1/5.67e9;

ep4 = efv + (ei-ef)./(1+(2*pi*f4).^2*tau^2);

part1 = ((ei-ef)*2*pi*tau.*f4);
part2 = (1+(2*pi*f4).^2*tau^2);
part3 = con./(2*pi*f4*e0);
epp4 = part1./part2 + part3;
Kz = [ ];
for m = 1:7

part1 = (2*pi*f4).^2*u0*e0.*ep4;
part2 = ((m*pi)^2)/a^2*ones(1,sizefreq4);
part3 = j*(2*pi*f4).^2*u0*e0.*epp4;

temp= sqrt(part1-part2-part3);
Kz = [Kz; temp];
end

imp1 = exp(-j*Kz(1,:)*L);
imp2 = exp(-j*Kz(2,:)*L);
imp3 = exp(-j*Kz(3,:)*L);
imp4 = exp(-j*Kz(4,:)*L);
imp5 = exp(-j*Kz(5,:)*L);
imp6 = exp(-j*Kz(6,:)*L);
imp7 = exp(-j*Kz(7,:)*L);

Calc4 = 8.686*log(abs(constants(1)*imp1 +
constants(2)*imp3 + constants(3)*imp5 + constants(4)*imp7
- constants(5)*imp2- constants(6)*imp4-
constants(7)*imp6));

f=test1(:,1)';
if flag == 1
    subplot(4,1,1)
    plot(f1,Calc1,'b',f1,test1(:,2),'r');
    subplot(4,1,2)
    plot(f2,Calc2,'b',f2,test2(:,2),'r');
    subplot(4,1,3)
    plot(f3,Calc3,'b',f3,test3(:,2),'r');
    subplot(4,1,4)
    plot(f4,Calc4,'b',f4,test4(:,2),'r');
    axis([0 max(f1) -150 0]);

```

```

    pause(.01)
end

error1 = sum((Calc1-test1(:,2)')).^2); % outputs the summed
squared error of the real answer and the found answer

error2 = sum((Calc2-test2(:,2)')).^2); % outputs the summed
squared error of the real answer and the found answer

error3 = sum((Calc3-test3(:,2)')).^2); % outputs the summed
squared error of the real answer and the found answer

error4 = sum((Calc4-test4(:,2)')).^2); % outputs the summed
squared error of the real answer and the found answer

error = (error1/length(Calc1) + error2/length(Calc2) +
error3/length(Calc3))+ error4/length(Calc4);

```

Mode_swarm

```

function constants = mode_swarm(test1, test2, test3,
test4)
% test1 is water reference, test2 is isopropyl alcohol
reference, test3 is air reference
% This is the ground truth or the final answer that we
are trying to find.
agents = 50;
pos = (rand(agents,7)); % creates initial positions of
particls ( 30 by 7)

vel = .25*(rand(agents,7)-.5); % creates a matrix of 30 by
7 of random values, initial velocities
pbpos = pos; % the personal bests are where the particles
initial positions.
pb = zeros(agents,1);

gbpos = pos(1,:);

% remove noisy data
test_no_noise = find(test1(:,2) > -80);
noiseless = test1(test_no_noise,2);
noiselessf = test1(test_no_noise,1);
test1 = [noiselessf noiseless];

% remove noisy data
test_no_noise = find(test2(:,2) > -80);

```

```

noiseless = test2(test_no_noise,2);
noiselessf = test2(test_no_noise,1);
test2 = [noiselessf noiseless];

% remove noisy data
test_no_noise = find(test3(:,2) > -80);
noiseless = test3(test_no_noise,2);
noiselessf = test3(test_no_noise,1);
test3 = [noiselessf noiseless];

% remove noisy data
test_no_noise = find(test4(:,2) > -80);
noiseless = test4(test_no_noise,2);
noiselessf = test4(test_no_noise,1);
test4 = [noiselessf noiseless];

% fills the personal best matrix for each agent.
for i=1:agents
    pb(i)= mode_fitness(pos(i,:),test1, test2, test3,
test4,0);
end
% searches the personal best matrix to find the global
best.
gb = pb(1); %initialize the global best to the first value
in the personal best matrix
for i=1:agents
    if pb(i)<gb % if the personal best of that agent is
better (less) than the global, reset the global.
        gb=pb;
        gbpos=pbpos(i,:);
    end
end
trash = mode_fitness(gbpos,test1, test2, test3,test4,1) ;

for i=1:400 % number of iterations or times that the
agents will move.
    temp = repmat(gbpos,agents,1); % create global best
postion matrix of 30.
    pos = pos + vel; % update equations for next
position
    vel = vel + .1*rand(1)*(pbpos-pos) +
.05*rand(1)*(temp-pos); % update equation for next
velocity.

    for j=1:agents % for each agent
        error = mode_fitness(pos(j,:),test1, test2,
test3,test4,0); % run to find the error
    end
end

```

```

        if error < pb(j)
            pbpos(j,:) = pos(j,:); % if error is less, it
stores that position as the new personal best position.
            pb(j) = error;
        end

        if error < gb
            gbpos = pos(j,:); % tests for the global best
and sets that to be the new global best postions.
            gb = error;
            trash = mode_fitness(gbpos,test1, test2,
test3,test4,1) ;
        end
    end

end

constants = gbpos;

```

Cal_fitness

```

function error = cal_fitness(constants, dimensions, test1,
flag)
% test one is water, test 2 is Isopropyl alcohol, test 3
is Air

f1=test1(:,1)';

% parallel plate dimensions in inches
a = dimensions(1); %1.875;
L = dimensions(2); %4;

sizefreq1 = length(f1);
e0 = 8.854187817e-12;
u0 = 4*pi*1e-7;
a = a*.0254;
L = L*.0254;

% begin Water
con = 1000e-5; % in Siemens/meter
ei = 78.982;
efv = 4.9*ones(1,sizefreq1);
ef= 4.9;
tau = 8.309e-12;

```

```

ep1 = efv + (ei-ef)./(1+(2*pi*f1).^2*tau^2);

part1 = ((ei-ef)*2*pi*tau.*f1);
part2 = (1+(2*pi*f1).^2*tau^2);
part3 = con./(2*pi*f1*e0);
eppl = part1./part2 + part3;
Kz = [ ];
for m = 1:7

part1 = (2*pi*f1).^2*u0*e0.*ep1;
part2 = ((m*pi)^2)/a^2*ones(1,sizefreq1);
part3 = j*(2*pi*f1).^2*u0*e0.*eppl;

temp= sqrt(part1-part2-part3);
Kz = [Kz; temp];
end

imp1 = exp(-j*Kz(1,:)*L);
imp2 = exp(-j*Kz(2,:)*L);
imp3 = exp(-j*Kz(3,:)*L);
imp4 = exp(-j*Kz(4,:)*L);
imp5 = exp(-j*Kz(5,:)*L);
imp6 = exp(-j*Kz(6,:)*L);
imp7 = exp(-j*Kz(7,:)*L);

Calc1 = 8.686*log(abs(constants(1)*imp1 +
constants(2)*imp3 + constants(3)*imp5 + constants(4)*imp7
- constants(5)*imp2- constants(6)*imp4-
constants(7)*imp6));

f=test1(:,1)';
if flag == 1
    % subplot(4,1,1)
    plot(f1,Calc1,'b',f1,test1(:,2),'r');

    pause(.01)
end

error1 = sum((Calc1-test1(:,2)').^2); % outputs the summed
squared error of the real answer and the found answer

error = error1/length(Calc1) ;

```

Cal_swarm

```

function dimensions = cal_swarm(mode_coeff, test1,
dielectric_ref)
% test1 is water reference, test2 is isopropyl alcohol
reference, test3 is air reference
% This is the ground truth or the final
% answer that we are trying to find.
agents = 8;

startpoint = [1.875 4];

pos = repmat(startpoint,agents,1).*(2*rand(agents,2)-.5);
vel = repmat(startpoint,agents,1).*(.25*(rand(agents,2)-
.5));

pbpos = pos; % the personal bests are where the particles
initial positions.
pb = zeros(agents,1);

gbpos = pos(1,:);

% remove noisy data
test_no_noise = find(test1(:,2) > -80);
noiseless = test1(test_no_noise,2);
noiselessf = test1(test_no_noise,1);
test1 = [noiselessf noiseless];

% fills the personal best matrix for each agent.
for i=1:agents
    pb(i)= cal_fitness(mode_coeff, pos(i,:),test1,0);
end
% searches the personal best matrix to find the global
best.
gb = pb(1); %initialize the global best to the first value
in the personal best matrix
for i=1:agents
    if pb(i)<gb % if the personal best of that agent is
better (less) than the global, reset the global.
        gb=pb;
        gbpos=pbpos(i,:);
    end
end
end
trash = cal_fitness(mode_coeff, gbpos, test1, 1) ;

```

```

for i=1:100 % number of iterations or times that the
agents will move.
    temp = repmat(gbpos,agents,1); % create global best
postion matrix of 30.
    pos = pos + vel; % update equations for next
position
    vel = vel + .05*rand(1)*(pbpos-pos) +
.01*rand(1)*(temp-pos); % update equation for next
velocity.

    for j=1:agents % for each agent
        error = cal_fitness(mode_coeff, pos(j,:),test1,
0); % run to find the error
        if error < pb(j)
            pbpos(j,:) = pos(j,:); % if error is less, it
stores that position as the new personal best position.
            pb(j) = error;
        end

        if error < gb
            gbpos = pos(j,:); % tests for the global best
and sets that to be the new global best postions.
            gb = error;
            trash = cal_fitness(mode_coeff, gbpos,test1,
1) ;
        end
    end
end

f=test1(:,1)';
a = gbpos(1); % originally 1.875
L = gbpos(2); %originally 4
a = a*.0254;
L = L*.0254;
sizefreq = length(f);
u0 = 4*pi*1e-7;
e0 = 8.854187817e-12;

con = 1000e-5;
ei = 78.982;
ef= 4.9;
tau = 8.309e-12;

efv = ef*ones(1,sizefreq);
ep = efv + (ei-ef)./(1+(2*pi*f).^2*tau^2);

```

```

part1 = ((ei-ef)*2*pi*tau.*f);
part2 = (1+(2*pi*f).^2*tau^2);
part3 = con./(2*pi*f*e0);
epp = part1./part2 + part3;

% Plot the original and experimental data.
plot(dielectric_ref(:,1),dielectric_ref(:,2),'r',f,ep,'b')

dimensions = gbpos;

```

Iterative_debye_swarm

```

function [t_ep, t_epp debeye] =
iterative_debye_swarm(test_rect, test_dielectric, Coeff3,
numruns, fit_type)
% This function returns two vectors, the real and
imaginary part of
% permittivity. Before using this data, the user should
be sure to load the
% required explosion_variables.mat file found in this
same directory. Inside this file are
% example waveforms and data, required calibrated
variables for this lab instrument as well
% as referenced dielectrics to be used to compare to
test samples.
% There are four parameters to be supplied by the user:
%
% An example function call is as follows:
%     >> iterative_debye_swarm(test_rect, test_ref,
Coeff3, numruns)
%
% test_rect is a matrix with the first column frequency
data and the
% second column as data from the rectangular
waveguide. This data
% should be easily imported from the VNA from a .xls
file by use of
% the 'import' command from matlab.
%
% test_ref is a matrix of reference data that the user
would like to
% compare to the output of the rectangular swarm.
Examples of common
% reference materials may be used from the
explosion_variables.mat

```



```

%      file.
%
%      Coeff3 is the vector of calibrated mode coefficients
from the
%      mode swarm software.  If simply using this as a
lab instrument, the
%      Coeff3 vector is included in the
explosion_variables.mat file
%
%      numruns is the number of swarm iterations the user
would like to run on
%      the swarm. 5 is an absolute minimum and 15 is
suggested. More than
%      this should not be required.
%
%      fit_type describes the type of fit that you would like
to use in the
%      calculation of the fitness function.  If you
choose fit_type=1, a
%      normal Cole-Cole with conductivity will be used.
If you choose
%      fit_type = 0, the conductivity will be set to zero
and stay at
%      zero.

debeye = [];
f=test_rect(:,1)';
for i=1:numruns
debeye = [debeye; debeye_swarm(Coeff3,test_rect,
fit_type)]
i
end
medEf = median(debeye(:,2))
stdev = std(debeye(:,2))

i = 1;
while(i <= numruns)
    if (( debeye(i,2) > (medEf + stdev)) | (debeye(i,2) <
(medEf-stdev) ))
        debeye(i,:) = [];
        numruns = numruns-1;
        i = i - 1;
    end
    i = i + 1;
end
avgEf = mean(debeye(:,2))
stdev = std(debeye(:,2))

```

```

i = 1;
while(i <= numruns)
    if (( debeye(i,2) > (avgEf + stdev)) | (debeye(i,2) <
    (avgEf-stdev) ))
        debeye(i,:) = [];
        numruns = numruns-1;
        i = i - 1;
    end
    i = i + 1;
end

```

```

avgEf = mean(debeye(:,2))
stdev = std(debeye(:,2))

```

```

i = 1;
while(i <= numruns)
    if (( debeye(i,2) > (avgEf + stdev)) | (debeye(i,2) <
    (avgEf-stdev) ))
        debeye(i,:) = [];
        numruns = numruns-1;
        i = i - 1;
    end
    i = i + 1;
end

```

```

debeye
avgEf = mean(debeye(:,2))
stdev = std(debeye(:,2))
figure;
for i=1:numruns
    dielectric_plot(test_rect,debeye(i,:), test_dielectric);
end

```

```

figure;

```

```

ep = [];
epp = [];
for i = 1:numruns
    [t_ep, t_epp] = debeye_plot(debeye(i,:), test_rect);

```

```

ep = [ep; t_ep];
epp = [ epp; t_epp];
end
final_ep = [];
final_epp = [];

```

```

for i = 1:length(test_rect)

    final_ep(i) = mean(ep(:,i));
    final_epp(i) = mean(epp(:,i));
end

subplot(2,1,1)
% plot for epsilon Prime
plot(f,final_ep,'b', test_dielectric(:,1),
test_dielectric(:,2),'r');
%plot(f,t_ep,'b', f,ep,'r');
hold on;

subplot(2,1,2)
%plot for epsilon double prime
plot(f,final_epp,'b', test_dielectric(:,1),
test_dielectric(:,3),'r')

```

Average_trans

```

function num2 = average_trans(test)
num = 0;
for i = 1:length(test)
    num = test(i,2) + num;
end

num2 = num/length(test);

```

Debye_fitness

```

function error = debeye_fitness(constants, parameters,
test, flag, fit_type)

f=test(:,1)';

% parallel plate dimensions in inches
a = 1.7634; % originally 1.875
L = 4.6069; %originally 4
a = a*.0254;
L = L*.0254;
sizefreq = length(f);
u0 = 4*pi*1e-7;
e0 = 8.854187817e-12;

```

```

con = constants(1);
ei = constants(2);
ef= constants(3);
tau = constants(4);
num = constants(5);

%if fit_type = 1 then do the normal Cole-cole type
%if fit_type is not 1 then remove the conductivity
if fit_type == 1

    efv = ef*ones(1,sizefreq);
    ep = efv + (ei-ef)./(1+(2*pi*f).^2*tau^2)+num;

    part1 = ((ei-ef)*2*pi*tau.*f);
    part2 = (1+(2*pi*f).^2*tau^2);
    part3 = con./(2*pi*f*e0);
    epp = part1./part2 + part3;
    Kz = [ ];
    for m = 1:7

        part1 = (2*pi*f).^2*u0*e0.*ep;
        part2 = ((m*pi)^2)/a^2*ones(1,sizefreq);
        part3 = j*(2*pi*f).^2*u0*e0.*epp;

        temp= sqrt(part1-part2-part3);
        Kz = [Kz; temp];
    end

else

    efv = ef*ones(1,sizefreq);
    ep = efv + (ei-ef)./(1+(2*pi*f).^2*tau^2)+num;

    part1 = ((ei-ef)*2*pi*tau.*f);
    part2 = (1+(2*pi*f).^2*tau^2);
    epp = part1./part2;
    Kz = [ ];
    for m = 1:7

        part1 = (2*pi*f).^2*u0*e0.*ep;
        part2 = ((m*pi)^2)/a^2*ones(1,sizefreq);
        part3 = j*(2*pi*f).^2*u0*e0.*epp;

        temp= sqrt(part1-part2-part3);
        Kz = [Kz; temp];
    end
end

```

```

end
imp1 = exp(-j*Kz(1,:)*L);
imp2 = exp(-j*Kz(2,:)*L);
imp3 = exp(-j*Kz(3,:)*L);
imp4 = exp(-j*Kz(4,:)*L);
imp5 = exp(-j*Kz(5,:)*L);
imp6 = exp(-j*Kz(6,:)*L);
imp7 = exp(-j*Kz(7,:)*L);

% Adjust parameters to use imaginary constants, if only
real constants, comment out.
%parameters(1) = parameters(1) + j*parameters(2);
% parameters(2) = parameters(3) + j*parameters(4);
% parameters(3) = parameters(5) + j*parameters(6);
% parameters(4) = parameters(7) + j*parameters(8);
% parameters(5) = parameters(9) + j*parameters(10);
% parameters(6) = parameters(11) + j*parameters(12);
% parameters(7) = parameters(13) + j*parameters(14);

Calc = 8.686*log(abs(parameters(1)*imp1 +
parameters(2)*imp3 + parameters(3)*imp5 +
parameters(4)*imp7 - parameters(5)*imp2-
parameters(6)*imp4- parameters(7)*imp6));

if flag == 1
    plot(f,Calc,'b',f,test(:,2),'r');
    axis([min(f) max(f) min(test(:,2)) 0]);
    xlabel('Frequency (Hz)');
    ylabel('dB');
    pause(.01)
end
firstquart = round(.2*sizefreq);
lastpart = sizefreq-firstquart;
error1 = sum((Calc(1:firstquart)-
test(1:firstquart,2)').^2);
error2 = sum((Calc(1:lastpart)-test(1:lastpart,2)').^2);

error = 2.5*error1 + error2;

```

Debeye_swarm

```

function constants = debeye_swarm(parameters, test,
fit_type) % constants was output
agents = 10;

startpoint1 = [3.1e-4 24.7 4.5 1/5.67e9 0]; % ethanol
startpoint
startpoint2 = [1000e-5 78.982 4.9 8.309e-12 0]; % water
startpoint
% remove noisy data
test_no_noise = find(test(:,2) > -60);
noiseless = test(test_no_noise,2);
noiselessf = test(test_no_noise,1);
test = [noiselessf noiseless];

if fit_type ~= 1
    startpoint1(1) = 0;
    startpoint2(1) = 0;
end

average_transmission = average_trans(test);

if( average_transmission > -50)

    %repeat matrix
    pos = repmat(startpoint2,agents,1).*(2*rand(agents,5));
    vel = repmat(startpoint2,agents,1).*(.25*(rand(agents,5)-
.5));

else

    %repeat matrix
    pos = repmat(startpoint1,agents,1).*(2*rand(agents,5));
    vel = repmat(startpoint1,agents,1).*(.25*(rand(agents,5)-
.5));

end

pbpos = pos;
pb = zeros(agents,1);

gbpos = pos(1,:);

%initialization of personal best and global best
matricies.
for i=1:agents

```

```

        pb(i)=debeye_fitness(pos(i,:), parameters, test, 0,
fit_type);
end

gb = pb(1);
for i=1:agents
    if pb(i)<gb
        gb=pb;
        gbpos=pbpos(i,:);
    end
end
trash = debeye_fitness(gbpos, parameters, test, 1,
fit_type) ;
%the actual swarm begins here
for i=1:100
    temp = repmat(gbpos,agents,1);
    pos = pos + vel;
    vel = vel + .1*rand(1)*(pbpos-pos) +
.05*rand(1)*(temp-pos);

    for j=1:agents
        error = debeye_fitness(pos(j,:), parameters, test,
0, fit_type);
        if error < pb(j)
            pbpos(j,:) = pos(j,:);
            pb(j) = error;
        end

        if error < gb
            gbpos = pos(j,:);
            gb = error;
            trash = debeye_fitness(gbpos, parameters,
test, 1, fit_type) ;
        end
    end
end

end
%this is the first noise injection (explosion)
vel = vel + 10*randn(1)*pos;
for i=1:200
    temp = repmat(gbpos,agents,1);
    pos = pos + vel;
    vel = vel + .1*rand(1)*(pbpos-pos) +
.05*rand(1)*(temp-pos);

    for j=1:agents

```

```

        error = debeye_fitness(pos(j,:), parameters, test,
0, fit_type);
        if error < pb(j)
            pbpos(j,:) = pos(j,:);
            pb(j) = error;
        end

        if error < gb
            gbpos = pos(j,:);
            gb = error;
            trash = debeye_fitness(gbpos, parameters,
test, 1, fit_type) ;
        end
    end

end

vel = vel + 20*randn(1)*pos;
for i=1:300
    temp = repmat(gbpos,agents,1);
    pos = pos + vel;
    vel = vel + .1*rand(1)*(pbpos-pos) +
.05*rand(1)*(temp-pos);

    for j=1:agents
        error = debeye_fitness(pos(j,:), parameters, test,
0, fit_type);
        if error < pb(j)
            pbpos(j,:) = pos(j,:);
            pb(j) = error;
        end

        if error < gb
            gbpos = pos(j,:);
            gb = error;
            trash = debeye_fitness(gbpos, parameters,
test, 1, fit_type) ;
        end
    end

end

end
constants = gbpos;

```


BIBLIOGRAPHY

- [1] Richard G. Geyer, "Dielectric Characterization and Reference Materials," *Technical Note 1338*, National Institute of Standards and Technology, April 1990.
- [2] A. von Hippel, ed, *Dielectric Materials and Applications*, Boston: Artech House, 1898.
- [3] J. P. Rung and J. J. Fitzgerald, ed, *Dielectric Spectroscopy of Polymeric Materials: Fundamentals and Applications*, Washington DC: American Chemical Society, 1997.
- [4] P. Becher, *Encyclopedia of Emulsion Technology*, New York: Marcel Dekker, inc., 1983.
- [5] M.A. Stuchly, T.W. Athey, G.M Samaras and G. E. Taylor. "Measurement of Radio Frequency Permittivity of Biological Tissues with an Open-Ended Coaxial Line: Part II – Experimental Results," *MTT -30*, Vol. 1, Jan. 1982.
- [6] O. Sipahioglu, S.A. Barringer, I. Taub, and A.P.P. Yang. "Characterization and Modeling of Dielectric Properties of Turkey Meat," *JFS: Food Engineering and Physical Properties*, vol. 68, no. 2, 2003, pp. 521-527.
- [7] Andrzej Kraszewski, ed., *Microwave Aquametry: Electromagnetic Wave Interaction with Water-Containing Materials*, New York: IEEE Press, 1996.
- [8] Xiangjun Liao, G.S.V. Raghavan, Jinming Dai, and V.A. Yaylayan, "Dielectric properties of α -D-glucose aqueous solutions at 2450 MHz," *Food Research International*, vol. 19, no. 3, November 2003, pp. 209-21.
- [9] A J. Surowiec, S. S. Stuchly, "Dielectric Properties of Breast Carcinoma and the Surrounding Tissue," *IEEE Trans. On Biomedical Engineering*, vol. 35, no. 4, April 1988.
- [10] *Basics of Measuring the Dielectric Properties of Materials*, Agilent Technologies Application Note, April, 2005 [Online]. Available: <http://cp.literature.agilent.com/litweb/pdf/5989-2589EN.pdf>.
- [11] James Baker-Jarvis et al, "Improved Technique for Determining Complex Permittivity with the Transmission/Reflection Method," *IEEE Trans. MTT*, vol. 38, no. 8, Aug. 1990.

- [12] National Physics Library, *A Guide to the Characterization of Dielectric Materials at RF and Microwave Frequencies*, London: The Institute of Measurement and Control, 2003.
- [13] James Baker-Jarvis, "Transmission / Reflection and Short-Circuit Line Permittivity Measurements," *Technical Note 1341*, National Institute of Standards and Technology, July 1990.
- [14] W. P. Westphal, "Techniques of measuring the permittivity and permeability of liquids and solids in the frequency range 3 c/s to 50 kmc/s," *Tech. Rep. XXXVI*, Laboratory for Insulation Research, Massachusetts Institute of Technology, 1950 pp. 99-104.
- [15] H. Bussey, "Measurements of the RF properties of materials: A survey," *Proc. IEEE*, vol. 55, pp. 1046-1053, June 1967.
- [16] H.E. Bussey and J. E. Gray, "Measurement and standardization of dielectric samples," *IRE Trans. Instrum.*, vol. 1-11, no.3, , Jan. 1989,pp.244-252.
- [17] U. Raveendranath, "Broadband Coaxial Cavity Resonator for Complex Permittivity Measurement of Liquids", *IEEE Trans. IM*, vol. 49, no.6, Dec. 2000.
- [18] Shuh-Han Chao. "Measurements of Microwave Conductivity and Dielectric Constant by the Cavity Perturbation Method and Their Errors", *IEEE Trans. MTT*, vol. 33, no. 6, June 1985.
- [19] R. A. Waldron. *The Theory of Waveguides and Cavities*. London: Maclaren and Sons, 1967.
- [20] R. G. Carter, "Accuracy of Microwave Cavity Perturbation Measurements," *IEEE Trans. MTT*, vol. 49, no. 5, May 2001, p. 918.
- [21] S.S Stuchly and M.A. Stuchly, "Coaxial line reflection method for measuring dielectric properties of biological substances at radio and microwave Frequencies, a review" *IEEE Trans. IM.* , vol 29, no.3, pp 176-183.
- [22] Gershon D. L., et al., "Open-Ended Coaxial Probe for High-Temperature and Broad-Band Dielectric Measurements," *IEEE Trans. on MTT*, vol. 47, no.9, 1999, pp 1640-1648.
- [23] *85070E Dielectric Probe Kit Datasheet: 200MHz to 50 GHz*, Agilent Technologies, Technical Overview, 2003.

- [24] Chen ChunPing, Chen MinYan, Yu JianPin, Niu Maode, and Xu Dering, "Uncertainty Analysis for the Simultaneous Measurement of Complex Electromagnetic Parameters Using an Open-ended Coaxial Probe," in *IEEE Proc. of IMTC Instrumentation and Measurement Technical Conference*, May, 2004, pp 61-65.
- [25] Ryusuke Nozaki and Tapan Bose, "Broadband Complex Permittivity Measurements by Time-Domain Spectroscopy," *IEEE Trans. Instrum. and Meas.*, vol. 39, no. 6, Dec. 1990, pp. 945-951.
- [26] Buford R. Jean, "Process Monitoring at Microwave Frequencies: A Waveguide Cutoff Method and Calibration Procedure," accepted for publication.
- [27] J. Kennedy and R. C. Eberhardt, "Particle swarm optimization," in *Proc. of the 1995 IEEE International Conference on Neural Networks*, vol. 4, pp. 1942-1948. IEEE Press, 1995.
- [28] R. D. Reed and R. J. Marks. *Neural Smoothing : supervised learning in feedforward artificial neural networks*. Cambridge, Mass.: The MIT Press, 1999.
- [29] *Agilent 8720E Family Microwave Vector Network Analyzers Datasheet*, Agilent Technologies, 2004.
- [30] A. P. Gregory and R. N. Clarke, "Traceable measurements of the static permittivity of dielectric reference liquids over the temperature range 5-50 °C," *Meas. Sci. Technol.*, vol. 16, 2005, pp. 1506-1516.
- [31] The reference materials section of the EMMA-club dielectrics database (CDROM) Release 1, 2001 (UK, NPL).
- [32] A.P Stogryn, H.T. Bull, K. Rubayi, and S. Iravanchy, "The Microwave Dielectric Properties of Sea and Fresh Water," GenCorp Aerojet, Sacramento, Calif., tech. rpt., 1995.
- [33] Floyd Buckley and Arthur A. Maryott, *Tables of Dielectric Dispersion Data for Pure Liquids and Dilute Solutions*, National Bureau of Standards Circular 589, Washington DC, Nov. 1958.
- [34] H Kienitz and K N Marsh, "Recommended reference materials for relaxation of physiochemical properties," *Pure Appl. Chem.*, vol. 53, pp1847-62, 1981.
- [35] B. P. Jordan, R. J. Sheppard and S. Szwarnowski, "The dielectric properties of formamide, ethanediol and methanol," *J. Phys. D: Appl. Phys.*, vol. 11, pp 695-701, 1978.

- [36] G. P. Cunningham, G. A. Vidulich and R. L. Kay, "Several properties of acetonitrile-water, acetonitrile-methanol and ethylene carbonate-water systems," *J. Chem. Eng. Data* 12, pp. 336-337, 1967.
- [37] D. R. Lide, ed. *Handbook of Chemistry and Physics*: 86th ed., New York: CRC Press,. 2005, pp. 6-132 to 6-136.
- [38] C. Inoue et. Al, "The Dielectric Property of Soybean Oil in Deep-Fat Frying and the Effect of Frequency," *Journal of Food Science*, vol. 67, no. 3, pp 1126-29, 2002.
- [39] G. Ciuprina, D. Loan, and L. Munteanu, "Use of intelligent-particle swarm Optimization in electromagnetics," *IEEE Tans. on Magnetics*, vol. 38 , pp.1037 – 1040, March 2002.
- [40] Wen Wang, Yilong Lu, J.S. Fu, and Yong Zhong Xiong, "Particle swarm optimization and finite-element based approach for microwave filter design," *IEEE Trans. on Magnetics*, vol. 41, no. 5, pp.1800 – 1803, May 2005.
- [41] D.W. Boerenger, D.H. Werner, "A comparison of particle swarm optimization and genetic algorithms for a phased array synthesis problem", *presented at Antennas and Propagation Society International Symposium*, June 22-27, 2003, pp. 181 -184.
- [42] Jacob Robinson and Yahya Rahmat-Samii," Particle Swarm Optimization in Electromagnetics, "*IEEE Trans. on Antennas and Propagation*, vol. 52, no. 2, Feb. 2004, 397-407.